

# FLT4 activation promotes chemoresistance in pediatric leukemia through stabilization of MDM2/MDMX and inactivation of p53

**Marion Dubuissez**

Centre de recherche de l'Hôpital Maisonneuve-Rosemont

**Djazia Haferssas**

Centre de recherche de l'Hôpital Maisonneuve-Rosemont

**Jonatan Barrera-Chimal**

Centre de recherche de l'Hôpital Maisonneuve-Rosemont

**Clémence Messmer**

Centre de recherche de l'Hôpital Maisonneuve-Rosemont

**El Bachir Affar**

Maisonneuve-Rosemont Hospital Research Center and Department of Medicine, University of Montréal

<https://orcid.org/0000-0002-6374-3683>

**Bruno Larrivé**

Maisonneuve-Rosemont Hospital Research Center and Department of Medicine, University of Montréal

**Xue-Song Liu**

ShanghaiTech University <https://orcid.org/0000-0002-7736-0077>

**Casimiro Gerarduzzi** (✉ [casimiro.gerarduzzi@umontreal.ca](mailto:casimiro.gerarduzzi@umontreal.ca))

Centre de recherche de l'H&#x00F4 <https://orcid.org/0000-0001-7098-1455>

---

## Article

**Keywords:** RTK, FLT4 (VEGFR-3), MDM2, MDMX, p53, chemotherapy resistance, pediatric leukemia

**Posted Date:** June 2nd, 2023

**DOI:** <https://doi.org/10.21203/rs.3.rs-2938071/v1>

**License:** © ⓘ This work is licensed under a Creative Commons Attribution 4.0 International License.

[Read Full License](#)

**Additional Declarations:** (Not answered)

---

1 **FLT4 activation promotes chemoresistance in pediatric leukemia through**  
2 **stabilization of MDM2/MDMX and inactivation of p53**

3  
4  
5 Marion Dubuissez<sup>1,2,3\*</sup>, Djazia Haferssas<sup>1,3\*</sup>, Jonatan Barrera-Chimal<sup>3</sup>, Clémence Messmer<sup>3,5</sup>,  
6 El Bachir Affar<sup>3,5</sup>, Bruno Larrivée<sup>1,4</sup>, Xue-Song Liu<sup>6</sup> and Casimiro Gerarduzzi<sup>1,3,4</sup>

7  
8  
9 <sup>1</sup> Département de pharmacologie et physiologie, Faculté de médecine, Université de Montréal,  
10 Québec, Canada

11 <sup>2</sup> Département de Microbiologie et Immunologie, Faculté de médecine, Université de Montréal,  
12 Québec, Canada

13 <sup>3</sup> Centre de Recherche de l'Hôpital Maisonneuve-Rosemont, Faculté de médecine, centre affilié à  
14 l'Université de Montréal, Québec, Canada

15 <sup>4</sup> Département de médecine, Faculté de médecine, Université de Montréal, Québec, Canada

16 <sup>5</sup> Département de Biochimie, Faculté de médecine, Université de Montréal, Québec, Canada

17 <sup>6</sup> School of Life Science and Technology, ShanghaiTech University, Shanghai, China.

18 \*Contributed Equally

19  
20 Key words: RTK, FLT4 (VEGFR-3), MDM2, MDMX, p53, chemotherapy resistance, pediatric  
21 leukemia.

22  
23 Running Title: FLT4 promotes p53 inactivation in Pediatric Leukemia

24  
25  
26 **\*Corresponding author:**

27 Casimiro Gerarduzzi  
28 Division of Nephrology, Maisonneuve-Rosemont Hospital CIUSSS de l'Est-de-l'Île-de-  
29 Montréal  
30 5415, boul. de l'Assomption  
31 Montréal, QC, Canada  
32 H1T 2M4  
33 Tel: 514-252-3400 ext:2813 [casimiro.gerarduzzi@umontreal.ca](mailto:casimiro.gerarduzzi@umontreal.ca)

34 **ABSTRACT**

35 Aberrant Receptor Tyrosine Kinase (RTK) signaling allows cancer cells to modulate  
36 survival, proliferation and death, leading to tumorigenesis and chemoresistance. In leukemia,  
37 the RTK FMS-Related Tyrosine Kinase 4 (FLT4) (also known as VEGFR-3, Vascular  
38 Endothelial Growth Factor- 3) is deregulated and correlates with cancer progression. However,  
39 the underlying consequences of its deregulation remain to be determined. Moreover,  
40 chemotherapy treatment requires that cancer cells retain a wild type p53 (wt) in order to respond  
41 to DNA damage by tumor suppressing activities, i.e. apoptosis. p53 activity is predominantly  
42 limited by its two major negative regulators, MDM2 and MDMX, which inactivate p53 by  
43 promoting its degradation and/or cytoplasmic localization. In this study, we have shown that  
44 activation of FLT4 by either overexpression or binding of its ligand, VEGF-C, leads to an  
45 increase in MDM2/MDMX stability, inactivation of p53 and resistance to DNA damaging  
46 therapies. Through immunoprecipitation and mass spectrometry analysis, we observed that  
47 FLT4 induced phosphorylation of MDMX at Ser-314, a consensus sequence of CDK4/6. Our  
48 data revealed that phosphorylation of MDMX on Ser-314 increases the stability of MDMX,  
49 which subsequently affects MDM2 and p53 degradation and could be reversed by the CDK4/6  
50 inhibitor Palbociclib. More importantly, leukemic cells treated with Palbociclib were more  
51 susceptible to DNA damaging induction of apoptosis and had reduced cell proliferation.  
52 Altogether, our research proposes an innovative way to reactivate p53 in pediatric leukemia  
53 through the pharmacological inhibition of FLT4 signaling, which could serve as a potential  
54 treatment option for this disease.

55 **ABBREVIATIONS:** AML, acute myeloid leukemia; ALL, acute lymphoid leukemia;  
56 CDK4/6, Cyclin Dependant Kinase 4/6; DLBC, Diffuse Large B Cell lymphoma; FLT4, FMS-  
57 Related Tyrosine Kinase 4; GFP, green fluorescent protein; IP, immunoprecipitation; MDM2,  
58 mouse double minute 2 homolog; MDMX, mouse double minute 4 homolog; MS/MS, mass

59 spectrometry; RTK, receptor tyrosine kinase; VEGF-C, vascular endothelial growth factor- C;  
60 VEGFR-3, vascular endothelial growth factor receptor-3; WB, Western Blot.

61

## 62 **INTRODUCTION**

63 Acute leukemia is a group of malignant disorders characterized by aberrant proliferation  
64 of hematopoietic stem cells and progenitors in the blood and bone marrow.<sup>1</sup> It is categorized  
65 into Acute Myeloid Leukemia (AML) and Acute Lymphoid Leukemia (ALL) according to the  
66 predominant type of cell involved. In adults, AML accounts for about 90% of all acute  
67 leukemias.<sup>2</sup> In contrast, ALL is the most common cancer in children.<sup>3</sup> In the pediatric  
68 population, chemotherapy treatments have achieved up to 90% remission.<sup>3,4</sup> However, the  
69 survival remains poor for 10% of these patients due to chemotherapy resistance.<sup>5,6</sup> Furthermore,  
70 effective doses can cause severe late effects of toxicity.<sup>7-9</sup> Therefore, a better understanding of  
71 these DNA-damaging therapies would permit precise treatments for leukemic cell death and  
72 lower dosages of effective treatments for reduced toxicity.

73 Most chemotherapies used in leukemia are DNA-damaging therapies<sup>10</sup> and therefore  
74 depend on activating the tumor suppressor p53 to induce tumor cell death. p53 was the first  
75 tumor suppressor to be identified and has been called the guardian of the genome due to its  
76 central role in preventing tumorigenesis. Indeed, p53 has multiple biological functions  
77 associated with tumor suppression, such as cell growth regulation, cell cycle arrest, DNA repair  
78 and apoptosis.<sup>11,12</sup>

79 The power of p53 in stress response is emphasized by its continual expression and  
80 degradation so that at any moment, p53 can be stabilized and positioned for its activity when  
81 needed. To avoid p53 lethality, two major negative regulators control its expression and  
82 activity, MDM2 (mouse double minute protein 2) and its homologous MDMX (mouse double  
83 minute 4 homolog, also known as MDM4).<sup>13</sup> MDM2 and MDMX regulate p53 activity by two

84 mechanisms.<sup>14</sup> First, the complex MDM2/MDMX binds to the transactivation domain of p53  
85 and prevents its activity as a transcription factor. Second, MDM2, unlike MDMX, has an E3  
86 ubiquitin ligase activity that can ubiquitinate p53 to be targeted for degradation by proteasomes.  
87 Therefore, p53 has a short half-life in normal conditions and is constantly expressed and  
88 degraded to be maintained at low levels. In response to stress signals such as DNA damage,  
89 p53 rapidly uncouples from the MDM2/MDMX complex allowing its stabilization and  
90 activation of tumor suppressing genes.<sup>14</sup>

91         Due to its essential role in preventing tumorigenesis, p53 is the most frequently mutated  
92 gene in human cancers, allowing tumor cell proliferation. Over 50% of solid tumors have p53  
93 mutations, most occurring in the DNA binding domain (DBD), altering its transcriptional  
94 activity.<sup>15</sup> However, the frequency of p53 mutations in hematological malignancies is lower.  
95 For instance, in pediatric leukemia, p53 mutations occur in less than 10% of patients and are  
96 associated with poor prognosis.<sup>16-19</sup> Thus, inactivation rather than mutation of p53 likely plays  
97 a role in leukemogenesis, and reactivation of the p53 pathway represents a potential target for  
98 improved treatment. Nevertheless, the precise mechanisms responsible for preventing wild type  
99 p53 function in leukemia remain unclear, indicating the potential involvement of inhibitory  
100 mechanisms upstream. Many cancers, including leukemia, overexpress MDM2 and MDMX.  
101 <sup>20-27</sup> In this context, the inhibition of MDM2/MDMX represents an attractive strategy to restore  
102 p53 functions.<sup>20</sup> Indeed, kinases activated by DNA damage inhibit MDM2 and MDMX, leading  
103 to p53 stabilization and activation.<sup>28,29</sup> Whether kinases involved in oncogenic signaling also  
104 target MDM2/MDMX for p53 regulation is still unclear.

105         Deregulating signaling pathways, including Receptor Tyrosine Kinase (RTK), is a  
106 hallmark of cancer.<sup>29,30</sup> Aberrant activation from RTKs allows cancer cells to abnormally  
107 control the cellular processes of survival, proliferation and cell death, leading to tumorigenesis  
108 and drug resistance.<sup>31</sup> Targeting aberrantly active RTKs in leukemia could therefore provide a

109 cotreatment approach to chemo/radiotherapy. Several findings have supported the role of the  
110 RTK FMS-Related Tyrosine Kinase 4 (FLT4, also called VEGFR-3 (Vascular Endothelial  
111 Growth Factor- 3)) and its ligand, VEGF-C, in cancer progression.<sup>32,33</sup> The VEGF family plays  
112 an essential role in angiogenesis during normal hematopoiesis.<sup>34</sup> Several findings have supported  
113 a role of the RTK FLT4 and its ligand, VEGF-C, in AML and ALL.<sup>30-32</sup> While FLT4 is not  
114 normally expressed in the bone marrow of healthy donors, both FLT4 and VEGF-C are  
115 expressed in more than one third of AMLs.<sup>30</sup> Specifically, AML cells from 96% of pediatric  
116 patients expressed detectable VEGF-C mRNA, while 49% expressed FLT4.<sup>33</sup> In a separate  
117 study, VEGF-C expression was associated with an adverse prognosis in pediatric and adult  
118 AML.<sup>34</sup> In pediatric ALL, VEGF-C protein was detected in 27% of patients, which was  
119 significantly associated with ALL treatment failure.<sup>32</sup> VEGF-C signaling has also been shown  
120 to play an important role in decreased drug response and chemotherapy resistance in acute  
121 leukemia.<sup>33-35</sup> Furthermore, *in vitro* VEGF-C treatment increased leukemic cell survival and  
122 proliferation<sup>34,35</sup>, and protected against apoptosis.<sup>34,35</sup> Although there is a strong association  
123 between FLT4 and leukemia, they have been understudied, and consequently, the mechanism  
124 by which FLT4 may be implicated in perpetuating leukemia and developing resistance to  
125 therapy is unknown.

126         Given that ALL patients have a wild type p53 and often have elevated levels of  
127 FLT4/VEGF-C, and resistance to DNA damage- induced apoptosis, we investigated whether the  
128 modulation of MDM2/MDMX complex sits at the interface of FLT4 and p53 activity. The  
129 present study shows that FLT4 leads to increased MDM2/MDMX complex stability, potentially  
130 through CDK4/6 and eventual p53 inactivation. We have also shown that reactivating p53 in  
131 FLT4-treated leukemic cells through CDK4/6 inhibition results in their responsiveness to  
132 genotoxic drugs promoting their apoptosis and thus providing a mechanism of combination  
133 therapy.

134

## 135 **MATERIAL AND METHODS**

### 136 **Cell culture**

137 The Human Embryonic Kidney cell line (HEK293T) and the Human Bone  
138 Osteosarcoma Epithelial cell line (U2OS) from American Type Culture Collection (ATCC)  
139 were seeded in tissue culture dishes and cultured until confluence in Dulbecco's Modified  
140 Eagle's Medium (DMEM, Gibco) supplemented with 10% of Foetal Bovine Serum (FBS,  
141 Gibco) and Penicillin/Streptomycin at 37°C in a humidified atmosphere of 5% CO<sub>2</sub>.

142 The human precursor B-ALL cell line (REH) from ATCC was seeded in 25 mL flasks  
143 and cultured until confluence in Roswell Park Memorial Institute media (RPMI 1640, Gibco)  
144 supplemented with 10% of FBS at 37°C in a humidified atmosphere of 5% CO<sub>2</sub>.

### 145 **Transient Transfections and Transductions**

146 Transient transfections were performed using Lipofectamine 2000 (Invitrogen)  
147 according to the manufacturer's instructions. The expression plasmids pCMV-Myc-MDM2,  
148 pCMV-MDM2 C464A mutant and pcDNA3-FLT4 were purchased from Addgene (#16441,  
149 #12086 and #119230 respectively). The expression plasmid pcDNA3-Flag-MDMX was  
150 previously described.<sup>36</sup> The expression plasmid pcDNA3-Flag-MDMX S314A mutant was  
151 generated using Quick Change II XL site-directed mutagenesis kit (Agilent Technologies) by  
152 two steps of site-directed PCR mutagenesis with the following primers:  
153 5'GTACTGAATGCAAGAAATTTAACGCTCCAAGCAAGAGGTACTG3' and  
154 3'CAGTACCTCTTGCTTGGAGCGTTAAATTTCTTGCATTCAGTAC5', according to the  
155 manufacturer's instructions.

156 The transduction was performed using lentivirus. First, HEK293T cells were seeded at  
157 50% of confluency. 24h after, cells were transfected using lipofectamine 2000 according to the  
158 manufacturer's instructions with plasmids for lentivirus production (3,74 µg psPAX2 + 1.25 µg

159 pMD2.G) and 6  $\mu$ g of lentiviral vectors pHAGE-GFP (control) or pHAGE-GFP-FLT4,  
160 purchased from Addgene (#12260, #12259 #106281 and #116745 respectively). After 48h of  
161 transfection, the supernatant containing the viral particles was collected and filtered using a  
162 0.45  $\mu$ m PVDF filter. For the transduction, REH cells were plated at  $1 \times 10^6$  cells/ mL in 2 ml of  
163 a completed medium, and 2 mL of filtrated supernatant supplemented with 4-8  $\mu$ g/mL of  
164 Polybrene (Sigma- Aldrich) was added to the cells. REH cells were centrifuged at 800 x g for  
165 30 min at 32°C. 48h after transduction, GFP-positive cells from each condition were sorted by  
166 Flow cytometry (BD ARIA III) and maintained in culture in completed media.

#### 167 **Colony Forming Assay of REH cells**

168 For each condition, 500 REH cells were resuspended in completed media and seeded in  
169 1mL of 1.2% methylcellulose (Stem Cell, #4230). Cells were plated in four replicates onto 35  
170 mm<sup>2</sup> tissue culture dishes and incubated in a humidified atmosphere at 37°C and 5% CO<sub>2</sub>. After  
171 two weeks of culture, colonies consisting of at least 50 cells were counted using an inverted  
172 microscope.

#### 173 **Growth Curve Analysis of REH cells**

174 For each condition, 100.000 REH cells were seeded in 6-well plate in 3 mL of complete  
175 media and treated or not with 1  $\mu$ M of CDK4/6 inhibitor (Palbociclib, Selleckchem). Cells were  
176 counted every 24h for five consecutive days.

#### 177 **FLT4 activation with VEGF-C**

178 For each condition, a total of  $1 \times 10^6$  REH cells were starved in 6-well plate in 3mL of  
179 starvation media overnight. The cells were treated with 100 ng/ mL of Recombinant Human  
180 VEGF-C (R&D Systems) or vehicle (H<sub>2</sub>O, control) at different time points. After the treatment,  
181 cells were harvested at 4°C, and the protein lysates were quantified and analyzed by Western  
182 Blot.

#### 183 **FLT4 inhibition with MAZ51**



184 For each condition, a total of  $1 \times 10^6$  REH cells were seeded in 6-well plate in 3 mL of  
185 starvation media a day before the treatment. The cells were then treated with 5  $\mu$ M of FLT4  
186 inhibitor (MAZ51, Sigma Aldrich) at different time points. After the treatment, cells were  
187 harvested at 4°C, and the protein lysates were quantified and analyzed by Western Blot.

#### 188 **Genotoxic treatment**

189 For each condition, a total of  $1 \times 10^6$  REH cells were seeded in 6-well plate in 3 mL of  
190 completed media a day before the treatment. The cells were treated with either 0.25  $\mu$ M of  
191 Etoposide (Sigma- Aldrich) or 50 nM Doxorubicin (Sigma-Aldrich) at different time points.  
192 After the treatment, cells were harvested at 4°C, and the protein lysates were quantified and  
193 analyzed by Western Blot.

#### 194 **FLT4 downstream signaling inhibitors**

195 For each condition, a total of  $1 \times 10^6$  REH cells were starved in 3 mL of starvation media  
196 in 6-well plate a day before the treatment. The cells were pre-treated with 2.5  $\mu$ M of CDK4/6  
197 inhibitor (Palbociclib, Selleckchem) for 24h. After the treatment, cells were harvested at 4°C,  
198 and the protein lysates were quantified and analyzed by Western Blot.

#### 199 **Whole-cell extracts preparation and Western Blot**

200 Total protein extracts were prepared from cells lysed by RIPA buffer (Pierce) containing  
201 a cocktail of protease and phosphatase inhibitors (Roche). The cell lysate was sonicated and  
202 centrifuged at 13.000 x g at 4°C. Proteins were quantified using Pierce BCA protein assay  
203 (Thermo Scientific). After quantification, proteins were denatured for 10 min at 95°C in  
204 Laemmli buffer. A total of 15-20  $\mu$ g of proteins from each condition were separated on SDS-  
205 PAGE using 10% acrylamide gels and transferred on 0,22  $\mu$ m PVDF membrane (BioRad). The  
206 membranes were blocked in 5% Non Fat Dry Milk (NFMD) in Tris buffered saline containing  
207 0.1% Tween (TBS-T) for 1h and incubated overnight at 4°C with the following primary  
208 antibodies: anti-MDM2 (86934S, Cell Signaling, 1:1000), anti-MDMX (3807946, Millipore,

209 1:1000), anti-FLT4 (3200622, Millipore, 1:1000), anti-phospho-Tyrosine- (9416S, Cell  
210 Signaling 1:1000), anti-p53 (Sc-126, Santa Cruz, 1:1000), and anti-GAPDH (9485, Abcam,  
211 1:1000). After primary antibodies incubation, membranes were washed during 30 min in TBS-  
212 T, and incubated with HRP- conjugated secondary antibodies: anti-mouse (Sc-516102, Santa  
213 Cruz, 1:2000) or anti-Rabbit (Sc-2357, Santa Cruz, 1:2000) during 1h at room temperature. The  
214 membranes were washed for 30 min and bands were detected with the Clarity Max Western  
215 ECL Substrate from Bio-Rad Laboratories (Hercules, USA). Results were analyzed by  
216 computer-assisted densitometry using ImageQuant LAS-4000 system from GE Healthcare Life  
217 Sciences (Mississauga, CAN) and FUJIFILM MultiGauge V3.0.

#### 218 **MDM2 immunoprecipitation and Mass Spectrometry analysis**

219       Following 24h of HEK293T transfection, cells were lysed in IP buffer (Tris 1M, pH=8,  
220 NaCl 5M, EDTA 0.5M, Nonidet P-40, 0.5%) containing a cocktail of proteases and phosphatase  
221 inhibitors (Roche) at 4°C. The cell lysate was sonicated and centrifuged at 13.000 x g at 4°C,  
222 and proteins were quantified using Pierce BCA protein assay (Thermo Scientific). After  
223 quantification, 1 mg of protein was incubated with 50 µL of Myc antibody- conjugated beads  
224 (Sigma- Aldrich) overnight at 4°C. After centrifugation, the supernatant was removed, and the  
225 beads were washed three times with IP buffer. The beads were then denatured for 10 min at  
226 95°C. The IP products were analyzed by Western Blot. MS-MS analysis was performed at  
227 Université de Montréal Mass Spectrometry platform (IRIC, Montréal, QC).

#### 228 **Flow cytometry analysis for apoptosis**

229       As previously described, REH cells were seeded until 80% confluency and treated with  
230 a gradient of genotoxic drugs (Doxorubicin or Etoposide). After 24h (Etoposide) or 48h  
231 (Doxorubicin), cells were washed three times with PBS and incubated at room temperature in  
232 Annexin V binding buffer (#42200, Biolegend,) containing APC-conjugated Annexin V  
233 antibody (#640919, Biolegend, 1:1000). After 15 min, Annexin V binding buffer containing

234 DAPI (#422801, Biolegend, 1:500) was added. Apoptosis was immediately measured by Flow  
235 cytometry using BD LSR Fortessa. Data analysis was performed using FlowJo Software.

### 236 **Dual luciferase assay**

237 U2OS were transfected either with FLT4 alone or in combination with MDM2 and  
238 MDMX as indicated, alongside with firefly Luciferase reporter plasmids (pGL3-Empty, pg13-  
239 p53 binding sites, pg13-mdm2 or pGL3-p21) that were described previously<sup>37</sup>. After 36h of  
240 transfection, cells were analyzed using the Dual-Luciferase Assay (Promega) according to the  
241 manufacturer's instructions. Renilla luciferase reporter plasmid under the control of the  $\beta$ -  
242 globin<sup>37</sup> was used to normalize the data.

### 243 **Immunofluorescence analysis for MDM2/MDMX complex**

244 24h post-transfection, cells were fixed with 4% paraformaldehyde and permeabilized in  
245 0.1% Triton-X-100/phosphate-buffered saline. Coverslips were incubated with primary  
246 antibody against MDM2 and MDMX, diluted in 1% BSA/phosphate-buffered saline overnight.  
247 After washing, coverslips were incubated in a secondary antibody, donkey anti-rabbit AF-647  
248 conjugated antibody (#711-605-152, Jackson ImmunoResearch Laboratories, 1:200) and  
249 donkey anti-mouse Cy-3 conjugated antibody (#715-165-150, Jackson ImmunoResearch  
250 Laboratories, 1:200) diluted in 1% BSA/phosphate-buffered saline for 1h. Coverslips were  
251 washed, and mounted with DAPI. Image acquisition was performed with Zeiss LSM880 multi-  
252 photon microscope and data were analyzed using Zeiss Blue software.

### 253 **Statistical analysis**

254 The results are expressed as mean  $\pm$  standard error. Statistical significance for multiple  
255 comparisons was calculated using ANOVA, while for two-group comparisons was calculated  
256 by a Student t-test. P-value  $< 0.05$  was considered statistically significant. Statistical analyses  
257 and graphical representation were performed using GraphPad Prism v6.07.

258

## 259 **RESULTS**

### 260 **Leukemia patients experience higher levels of FLT4 and VEGF-C expression**

261 We first analyzed the relationship between the expression of FLT4 and VEGF-C and  
262 the prognosis of leukemia patients. Using the GEPIA website tool<sup>38</sup>, we identified that the  
263 mRNA expression levels of FLT4 and VEGF-C were significantly upregulated in Diffuse Large  
264 B-cell Lymphoma (DLBC) patients as compared to normal datasets from the cancer genome  
265 atlas (TCGA) and the genotype tissue expression (GTEx) project (Fig. 1A). UALCAN  
266 database<sup>39</sup> analysis revealed that the FLT4 upregulation is significantly higher in stages 2 and  
267 4 of DLBC as compared to stage 1 (Fig. 1B).

### 268 **FLT4 overexpression negatively regulates p53 by promoting MDM2/MDMX complex**

269 Hematological malignancies have a relatively low frequency of TP53 mutations. We  
270 compared the frequency of p53 mutations amongst various leukemia public cohorts<sup>40-47</sup> in the  
271 cBio Cancer Genomics Portal (<http://cbioportal.org>) (Fig. 2A). The incidence of TP53  
272 mutations in DLBC and ALL (adult or pediatric) was around 20% in DLBC, and less than 10%  
273 in ALL in the total number of patients. Given the high wild type status of p53 in leukemia  
274 patients (Fig. 2A), we questioned if FLT4 overexpression may promote tumorigenicity by  
275 suppressing p53 activity. To gain this general mechanistic insight, we used a cell line harboring  
276 wild type p53, U2OS. We found a reduced p53 transcriptional activity in response to FLT4  
277 overexpression by using a p53-responsive luciferase reporter vector (Fig. 2B). To further  
278 validate the impact of FLT4 overexpression on reduced p53 activity, U2OS cells were  
279 transfected with luciferase reporters for p21 and MDM2, both of which have known p53-  
280 binding sites.<sup>48</sup> FLT4 overexpression had significantly decreased the transcriptional activity of  
281 p21 and MDM2 promoters (Fig. 2B). These results confirm the suppression of p53  
282 transcriptional activity and two p53 target genes, p21 and MDM2, by FLT4 overexpression.<sup>14</sup>

283 Our observed p53 suppression suggests that the mechanism of FLT4 may involve the  
284 transcription factor's key negative regulatory complex, MDMX and MDM2. We tested this  
285 hypothesis by transfecting various combinations of MDMX, MDM2 and FLT4 vector  
286 constructs and a p53 reporter vector in U2OS cells, followed by activating p53 activity through  
287 375  $\mu$ M 5'FU treatment. As expected, we show the suppression of p53 reporter activity by  
288 separate MDMX and MDM2 transfections, which had less of an impact individually than their  
289 co-expression (Fig. 2C). Interestingly, FLT4 overexpression was able to influence further the  
290 combined MDMX and MDM2 suppression of p53 activity.

291 MDMX and MDM2 are well known to stabilize each other from degradation when they  
292 form a heterodimer complex, which consequently accumulates to bind and suppress available  
293 p53. After identifying that FLT4 is able to co-modulate p53 activity through the  
294 MDM2/MDMX complex, we next studied the influence FLT4 had on stabilizing the complex.  
295 To assess this possibility, we transfected increasing amounts of FLT4 vector in HEK293T cells  
296 and measured endogenous MDM2 and MDMX expression. Interestingly, FLT4 overexpression  
297 increased endogenous MDM2 and MDMX proteins in a concentration-dependent manner,  
298 which correlated with an increasing amount of tyrosine phosphorylation (Figure 2D). Similar  
299 results were obtained in U2OS cells (Supp. Fig. 1). To further validate this, we transfected  
300 different combinations of vectors encoding MDM2, MDMX or FLT4 in HEK293T cells. Our  
301 data show that MDMX and MDM2 co-transfection increases MDM2 protein levels compared  
302 to an individual MDM2 transfection (Figure 2E). Moreover, the co-transfection of MDMX and  
303 MDM2 with FLT4 further induced the amount of MDM2.

304 FLT4 increase in MDM2 levels led us to evaluate if this effect would decrease p53  
305 protein levels and correlate with the lower levels of p53 activity. While co-transfection of  
306 MDM2 and MDMX was able to decrease p53 protein levels compared to their individual  
307 transfections, the addition of FLT4 to their co-transfection resulted in a further decrease in p53

308 levels (Fig. 2F). Therefore, the difference of MDM2 levels being inversely proportional to the  
309 amount of p53 was highest when FLT4 was co-transfected. To investigate whether the decrease  
310 in p53 was caused by increased ubiquitination from elevated MDM2, we tested the levels of  
311 p53 after transfection with an MDM2 mutant vector that is unable to ubiquitinate (MDM2  
312 C464A) using U2OS cells.<sup>49</sup> Although FLT4 was able to stabilize MDM2 C464A with MDMX,  
313 FLT4 had lost the ability to decrease the protein levels of p53 when compared to its co-  
314 transfection with wild type MDM2 and MDMX (Fig. 2G), implying the importance of the  
315 MDM2 ubiquitin ligase activity in FLT4-mediated decrease in p53.

316 Taken together, these results suggest that FLT4 overexpression strongly promotes the  
317 stabilization of the MDM2/MDMX complex, which subsequently leads to more MDM2 readily  
318 available to target p53 for degradation by ubiquitination and decreases its transcriptional  
319 activity.

#### 320 **FLT4 overexpression relocates the nuclear MDM2/MDMX complex to the cytoplasm**

321 To study the effect that FLT4 has on the localization of MDMX and MDM2, we co-  
322 transfected different combinations of MDM2, MDMX and FLT4 encoding vectors in U2OS  
323 cells and determined the localization of MDM2 and MDMX by immunofluorescence. As  
324 previously shown, MDMX alone was found in the cytoplasm, whereas MDM2 alone was  
325 localized in the nucleus.<sup>50</sup> When MDMX and MDM2 were co-expressed, MDMX relocated  
326 in the nucleus with MDM2 (Fig. 3). However, when FLT4 was overexpressed, we detected the  
327 MDM2/MDMX complex in the cytoplasm, suggesting that FLT4 was responsible for a  
328 localization shift of the heterocomplex. Our immunofluorescence results also confirmed the  
329 protein stability from our Western Blot studies, where MDM2 is stabilized by MDMX and  
330 furthermore by FLT4. Taken together, these results show that FLT4 overexpression promotes  
331 the stability of the MDM2/MDMX complex and relocates it in the cytoplasm.

332 **FLT4 induces phosphorylation of MDMX on Ser-314 to affect MDM2/MDMX**  
333 **heterodimerization**

334 Having shown that FLT4 overexpression induces an increase in the MDM2/MDMX  
335 complex, we aimed to investigate their molecular events. To substantiate the impact of FLT4  
336 on MDMX and MDM2, HEK293T cells were transfected with Myc-MDM2 and MDMX with  
337 or without FLT4 and then subjected to immunoprecipitation (IP) using Myc antibody-  
338 conjugated beads. As shown in Fig. 4A, the presence of FLT4 caused a greater pulldown of  
339 MDMX along with MDM2, suggesting a higher level of heterodimerization and subsequent  
340 stability of MDM2 (Fig. 4A). A Mass Spectrometry analysis (MS/MS) was performed on the  
341 IP products to identify phosphosites on either MDMX or MDM2, which may influence their  
342 heterodimerization. Interestingly, our data show that FLT4 overexpression induced  
343 phosphorylation of a serine residue on MDMX at position 314, Ser-314, which we have  
344 previously identified as a site involved in the MDM2/MDMX stability by two other RTKs,  
345 Her4 and Axl.<sup>36,51</sup> To validate if MDMX Ser-314 had the same impact on FLT4 signaling as  
346 our previous RTKs, we transfected HEK293T cells with a combination of FLT4 and MDM2  
347 vectors, and either a wild type MDMX or an MDMX mutant vector that contains a 314 Serine  
348 residue replaced with Alanine to impede its phosphorylation (MDMX S314A). Regardless of  
349 the combination of MDMX S314A, MDM2 and FLT4 co-expression, we observed a decrease  
350 in MDMX S314A stability compared to those transfections with wild type MDMX (Fig. 4B  
351 and Supp. Fig. 2), which consequently affected MDM2 levels. Furthermore, when Myc-MDM2  
352 was immunoprecipitated using Myc conjugated beads, we revealed that the Ser-314  
353 phosphosite affected the affinity between MDMX and MDM2, both with or without FLT4 co-  
354 transfections (Fig. 4C). This suggests that FLT4 induces phosphorylation of Ser-314 on  
355 MDMX, resulting in an increase in MDMX protein level that would be available to bind with  
356 MDM2. (Fig. 4C).

357 To investigate which kinase was responsible for the novel phosphorylation, we  
358 previously analyzed the MDMX Ser-314 site using the kinase prediction software GPS to  
359 identify potential candidates that mediate the FLT4 signal. The search criteria used were highly  
360 stringent, and the software identified CDK4/6 as a candidate kinase. To verify this prediction,  
361 HEK293T cells were pretreated with Palbociclib, a specific inhibitor for CDK4/6, which  
362 impeded the ability of FLT4 to stabilize the MDMX-MDM2 complex, as shown in Fig. 4D.

363 Therefore, our findings suggest that FLT4's oncogenic behavior is partly due to its  
364 ability to phosphorylate MDMX at Ser-314 in a CDK4/6-dependent manner. This results in  
365 increased stability of both MDMX and the MDMX-MDM2 heterocomplex, ultimately leading  
366 to p53 inactivation.

367 **Activation of FLT4 in leukemic cells stabilizes the MDM2/MDMX complex leading to p53**  
368 **decrease**

369 To add relevance to our overexpression experiments, we examined the impact of  
370 stimulating endogenous FLT4 on the signaling mechanisms found in leukemia. Specifically,  
371 we used the ALL cell line REH due to their wild type p53 and high FLT4 expression compared  
372 to other known ALL cell lines, which express a p53 mutant (Fig. 5A). To activate endogenous  
373 FLT4, we treated REH leukemic cells with 100 ng/mL of its ligand, VEGF-C, at different time  
374 points. FLT4 activity was measured through total tyrosine phosphorylation and evaluated for  
375 its potential effect on the stability of intracellular MDM2/MDMX and p53 levels. Over a span  
376 of about 3 hours, VEGF-C was able to stimulate total tyrosine phosphorylation as early as one  
377 hour, which corresponded to a gradual increase in MDMX and MDM2 and a decrease in p53  
378 levels (Fig. 5B and Supp. Fig. 3A). Interestingly, our 5min intervals of VEGF-C treatment  
379 revealed a cyclic increase in MDM2/MDMX followed by a decrease in p53, and vice versa. To  
380 confirm the effect of FLT4 on MDM2/MDMX complex, we treated the cells with a specific  
381 inhibitor of FLT4, MAZ51. A 30-minute pre-treatment with MAZ51 reversed the FLT4 effect



382 by decreasing MDM2 and MDMX as early as 30 min and restoring p53 levels (Fig. 5C and  
383 Supp. Fig. 3B).

384 To validate our results, we stably transduced FLT4 in REH cells. We similarly found  
385 FLT4 overexpression to increase the protein levels of MDMX and MDM2 while decreasing  
386 that of p53 (Fig. 5D). The CDK4/6 pathway was also implicated in the FLT4 stability of  
387 MDMX and MDM2 since Palbociclib reversed the effect (Fig. 5E).

388 Taken together, the influence of the FLT4-CDK4/6 pathway on MDM2/MDMX/p53  
389 axis is conserved within an *in vitro* leukemic model.

### 390 **The effect of FLT4 on MDM2/MDMX and p53 enhances cell survival and increased** 391 **resistance to chemotherapy**

392 After showing that FLT4 has the ability to stabilize the MDM2/MDMX complex, we  
393 aimed to investigate whether this impact of FLT4 on leukemic cells would have any  
394 implications on p53 cell death and response to DNA-damaging agents. First, we observed that  
395 the FLT4-induced REH cells led to an increase in cell proliferation (Fig. 6A) and colony  
396 formation (Fig. 6B). To assess the effect of FLT4 in response to DNA damage, we treated the  
397 REH overexpressing FLT4 cells with genotoxic drugs commonly used in the treatment of  
398 leukemia, Doxorubicin and Etoposide, for 5h and 3h respectively (Fig. 6C and 6F). The results  
399 showed that MDM2 was higher in cells overexpressing FLT4 as compared to the control.  
400 Furthermore, cells overexpressing FLT4 were shown to have lower levels of p53 in response to  
401 DNA damage in both genotoxic treatments (Fig. 6C and 6F). Since p53 regulates cell death, we  
402 studied the effects of a p53 decrease on apoptosis activation in response to DNA damage stress.  
403 After treatment with genotoxic drugs, we performed staining with Annexin V and DAPI and  
404 measured the amount of apoptosis. Interestingly, cells overexpressing FLT4 showed lower  
405 levels of apoptosis compared to the controls with both Doxorubicin and Etoposide (Fig 6D and  
406 6G), which was concentration-dependent (Fig. 6E and H).

407 Collectively, these results show that FLT4 activation increases the proliferation of  
408 leukemic cells. Furthermore, the constitutive activation of FLT4 decreases the sensitivity of  
409 leukemic cells to the DNA-damage induced- apoptosis, therefore increasing their survival.

#### 410 **Targeting CDK4/6 acts as a Therapeutic Strategy to Overcome FLT4-Induced** 411 **Chemoresistance in Leukemia**

412 As our main finding, we observed that FLT4 phosphorylation of a novel Ser-314 site on  
413 MDMX, mediated by CDK4/6, is partly responsible for the increased amount of the MDMX-  
414 MDM2 complex and subsequent decrease in p53. As a therapeutic option, we tested if blocking  
415 CDK4/6 could decrease the survival of FLT4 overexpressing leukemic cells and succumb them  
416 to DNA damaging therapy. First, we observed that the increased proliferation induced by FLT4  
417 overexpression on REH cells was significantly reduced by the pretreatment with the CDK4/6  
418 inhibitor, Palbociclib (Fig. 7A). Furthermore, Palbociclib was able to succumb FLT4-REH cells  
419 to a higher percentage of apoptosis in response to Doxorubicin (Fig. 7B).

420 In summary, our findings established that FLT4 exhibits its oncogenic properties by  
421 phosphorylating MDMX on Ser-314 in a manner dependent on CDK4/6. In turn, this leads to  
422 elevated stability of MDM2, which results in an increase in the MDMX-MDM2 heterocomplex,  
423 ultimately resulting in lower levels of p53 protein and activity, as illustrated in Figure 8.

424

#### 425 **DISCUSSION**

426 Chemotherapy depends on the activation of p53, a master regulator of cellular stress and  
427 DNA damage.<sup>11</sup> Disruption of p53 plays a role in the cell during cancer development and its  
428 response to DNA-damaging therapies. While p53 mutations are frequent in solid tumors, p53  
429 mutations occur in less than 10% of leukemia.<sup>19</sup> Thus, inactivation rather than mutations could  
430 play a role in the proliferation of leukemic cells and chemoresistance. Therefore, it is crucial to

431 understand the mechanisms of chemoresistance in leukemia to develop better and more  
432 effective treatments.

433 RTK deregulation is common in several cancers, allowing tumor cells to increase their  
434 proliferation and survival.<sup>29,52</sup> An understudied phenomena is the overexpression of the RTK  
435 FLT4 and its specific ligand VEGF-C in leukemia, as well as its association with treatment  
436 failure.<sup>30</sup> Interestingly, this association had been predominantly shown in pediatric acute  
437 lymphoid leukemia.<sup>3</sup> However, to date, the role of FLT4 in regulating p53 has not been studied.  
438 This suggests that the pro-survival pathway of FLT4 may be impeding the ability of p53 to  
439 suppress its tumor activity but also to respond to DNA damaging therapies. In this study, we  
440 provide evidence that the activation of FLT4 in leukemic cells, either through overexpression  
441 or VEGF-C stimulation, stabilizes and relocates MDM2 and MDMX into the cytoplasm and  
442 reduces the levels of p53. Additionally, we found that the ubiquitination activity of MDM2  
443 plays a crucial role in reducing p53 levels via FLT4. Since MDM2 and MDMX proteins are the  
444 main negative regulators of p53, these findings suggest that the cytoplasmic relocalization of  
445 MDM2/MDMX may be promoting the nuclear export of p53 for its ubiquitination-targeted  
446 degradation. Consequently, the decrease of p53 in leukemic cells correlated with an increase  
447 in the survival of leukemic cells under normal and genotoxic conditions, which resulted in a  
448 greater colony size. Hence, we provide a mechanism through FLT4 that contributes to  
449 tumorigenesis and response to DNA damage by modulating the MDM2/MDMX/p53 axis.

450 Under VEGF-C stimulation over short periods of time, oscillations in the stability of  
451 MDM2 and MDMX and p53 levels are observed possibly due to the dynamic interaction  
452 between p53 and MDM2. The tumor suppressor protein p53 is a master transcriptional regulator  
453 of the response of human cells to DNA damage. Upon cellular exposure to DNA damage, p53  
454 stabilization leads to the transcriptional induction of hundreds of genes involved in DNA repair,  
455 cell-cycle arrest, apoptosis, and cellular senescence.<sup>11</sup> In addition, p53 regulates the expression

456 of proteins involved in controlling its levels, including MDM2 and MDMX, which tags p53 for  
457 proteasomal-dependent degradation and consequently lower MDM2/MDMX expression.<sup>14</sup>  
458 This oscillatory dynamics of p53 inhibition generated by the interaction of p53 and MDM2  
459 creates a negative feedback loop. Therefore, VEGF-C stimulation of MDM2/MDMX stability  
460 will lead to p53 degradation, reducing the transcription of MDM2 and MDMX, which in turn  
461 positively upregulate p53 levels. The interaction of p53 and MDM2 generates oscillatory  
462 dynamics of p53 activation characterized by a stereotyped frequency and noisy amplitude.  
463 Fluctuations in the oscillatory pattern of p53 trigger a sharp switch between its activation and  
464 inhibition, leading to escape from cell-cycle arrest. Transient perturbation of p53 stability  
465 mimics the noise in individual cells and is sufficient to trigger escape from arrest.<sup>53</sup> Thus, self-  
466 reinforcing circuitry that mediates cell-cycle transitions can translate small fluctuations in p53  
467 signaling into large phenotypic changes of oncogenic propagation. In short, oscillations in the  
468 stability of MDM2 and MDMX and p53 levels are observed under VEGF-C stimulation over  
469 short periods due to the dynamic interaction between p53 and MDM2.

470 In order to dissect the molecular mechanisms of p53 regulation by FLT4, we performed  
471 a MS/MS analysis on the MDM2/MDMX complex. Interestingly, the phosphosite Ser-314 on  
472 MDMX was increased in the presence of FLT4. Ser-314 is located on the zinc finger domain  
473 of MDMX, a region that does not contact MDM2 and is known to play a role in kinase  
474 signaling.<sup>13</sup> This implies that the FLT4-mediated signal directly affects MDMX to indirectly  
475 affect MDM2, possibly regulating MDMX stability through phosphorylation. The same  
476 phosphosite was shown by our previous studies to be implicated in the stabilization of MDMX  
477 by the RTKs HER4 and AXL in the context of breast cancer and melanoma, respectively.<sup>36,51</sup>  
478 The importance of Ser-314 for the stability of MDMX in our new model of FLT4 was confirmed  
479 using a mutant MDMX, where the Serine 314 site was replaced by Alanine, which led to a  
480 reduction in MDMX and a loss in the FLT4-induced stabilization of the heterodimer complex.

481 One of the kinases predicted to be responsible for the phosphorylation of MDMX Ser-314 was  
482 CDK4/6, which is a master regulator of the cell cycle that regulates the critical checkpoint in  
483 the G1-S transition needed for the progression of the cell cycle.<sup>54</sup> It is noteworthy that certain  
484 cancers, including hematological malignancies, possess a functional CDK4/6 pathway  
485 alongside elevated levels of MDM proteins and retain a wild type p53 and that CDK4/6  
486 inhibitors can impede the cell cycle progression of cancerous cells. In fact, we observed that  
487 CDK4/6 inhibition reduced MDMX levels and increased susceptibility to apoptosis in FLT4-  
488 overexpressing cells.

489 While targeting RTKs with inhibitors has shown limited success as a strategy in cancer  
490 treatment, their effects on the p53 regulatory unit have not been fully explored therapeutically.  
491 Our findings suggest that the stabilization of the MDMX-MDM2 complex is the converging  
492 point of oncogenic signals, mediated by the activation of FLT4 and CDK4/6 kinase and leading  
493 to enhanced suppression of p53 activity. Our proposed model takes into account our results and  
494 the function of the MDMX zinc finger domain in transmitting kinase signaling. In our proposed  
495 model, the activation of CDK4/6 by FLT4 triggers the phosphorylation of MDMX at Ser-314,  
496 which causes it to undergo a conformational change that enhances its stability. Subsequently,  
497 MDMX binds to and stabilizes MDM2, which leads to the stabilization of the MDM2/MDMX  
498 complex and, as a consequence, inhibits the tumor suppression and DNA-damaging response  
499 of p53 by shuttling it to the cytoplasm and ubiquitinating it for degradation (Fig. 8).

500 In conclusion, ALL harbor a wild type p53 and often have elevated levels of  
501 FLT4/VEGF-C, correlating with poor prognosis. In addition, VEGF-C treated leukemic cells  
502 induce mitogenic effects and protect against apoptosis. It is possible ALL share a common  
503 mechanism of p53 suppression through the FLT4/VEGF-C axis to support their carcinogenic  
504 qualities and therapy resistance. For these reasons, our research proposes an innovative way to

505 reactivate p53 in pediatric leukemia through the pharmacological inhibition of FLT4 signaling  
506 as a novel treatment of pediatric leukemia.

507

#### 508 **AUTHOR CONTRIBUTION STATEMENT**

509 C.G. conceived and designed the experiments; M.D., D.H., C.M., and C.G. performed the  
510 experiments; M.D., D.H., J.B.C., and C.G. analyzed the results and wrote the manuscript;  
511 J.B.C., E.B.A., B.L., X.L., and C.G. discussed and analyzed the experiments; All authors read  
512 and approved the final manuscript.

#### 513 **FUNDING**

514 This work was supported by grants from the Cancer Research Society and the Kidney Cancer  
515 Research Network of Canada (co-funded Operating Grant Program #24347 to C. Gerarduzzi),  
516 and the Hôpital Maisonneuve-Rosemont Foundation (to C. Gerarduzzi). C. Gerarduzzi is a  
517 recipient of the Fonds de Recherche – Santé (Bourses de chercheurs-boursiers Junior 1  
518 #298956) and the Cole Foundation Early Career Transition Award (C.G). M.D. is the recipient  
519 of the Janssen Consortium Fellowship and D.H. is a recipient of the Cole Foundation PhD  
520 scholarship.

#### 521 **CONFLICT OF INTEREST**

522 The authors declare that they have no conflict of interest.

#### 523 **DATA AVAILABILITY**

524 All data generated or analyzed during this study are present in this published article. Any  
525 additional information pertinent to the data may be requested from the corresponding author.

526

527 **REFERENCES**

528

- 529 1. Ferrando AA, López-Otín C. Clonal Evolution in Leukemia. *Nature Medicine*. Nature  
530 Publishing Group; 2017.
- 531 2. Longo DL, Döhner H, Weisdorf DJ, et al. Acute Myeloid Leukemia. *The New England*  
532 *Journal of Medicine*. 2015.
- 533 3. Whitehead TP, Metayer C, Wiemels JL, et al. Childhood Leukemia and Primary  
534 Prevention. *Curr Prob Pediatr Ad* 2016;46(10):317–352; doi: 10.1016/j.cppeds.2016.08.004.
- 535 4. Maloney KW, Devidas M, Wang C, et al. Outcome in Children With Standard-Risk B-Cell  
536 Acute Lymphoblastic Leukemia: Results of Children’s Oncology Group Trial AALL0331.  
537 2019;38:602–612; doi: 10.1200/jco.19.
- 538 5. Schultz KR, Devidas M, Bowman WP, et al. Philadelphia chromosome-negative very high-  
539 risk acute lymphoblastic leukemia in children and adolescents: results from Children’s  
540 Oncology Group Study AALL0031. *Leukemia* 2014;28(4):964–967; doi:  
541 10.1038/leu.2014.29.
- 542 6. Nguyen K, Devidas M, Cheng S-C, et al. Factors influencing survival after relapse from  
543 acute lymphoblastic leukemia: a Children’s Oncology Group study. *Leukemia*  
544 2008;22(12):2142–2150; doi: 10.1038/leu.2008.251.
- 545 7. Winick NJ, Carroll WL, Hunger SP. Childhood Leukemia — New Advances and  
546 Challenges. *New Engl J Medicine* 2004;351(6):601–603; doi: 10.1056/nejme048154.
- 547 8. Oeffinger KC, Eshelman DA, Tomlinson GE, et al. Grading of late effects in young adult  
548 survivors of childhood cancer followed in an ambulatory adult setting. *Cancer*  
549 2000;88(7):1687–1695; doi: 10.1002/(sici)1097-0142(20000401)88:7<1687::aid-  
550 cncr24>3.0.co;2-m.
- 551 9. Essig S, Li Q, Chen Y, et al. Risk of late effects of treatment in children newly diagnosed  
552 with standard-risk acute lymphoblastic leukaemia: a report from the Childhood Cancer  
553 Survivor Study cohort. *Lancet Oncol* 2014;15(8):841–851; doi: 10.1016/s1470-  
554 2045(14)70265-7.
- 555 10. Madhusoodhan PP, Carroll WL, Bhatla T. Progress and Prospects in Pediatric Leukemia.  
556 *Curr Prob Pediatr Ad* 2016;46(7):229–241; doi: 10.1016/j.cppeds.2016.04.003.
- 557 11. Bieging KT, Mello SS, Attardi LD. Unravelling Mechanisms of P53-Mediated Tumour  
558 Suppression. *Nature Reviews Cancer*. Nature Publishing Group; 2014.
- 559 12. Ashcroft M, Vousden KH. Regulation of p53 stability. *Oncogene* 1999;18(53):7637–  
560 7643; doi: 10.1038/sj.onc.1203012.
- 561 13. Wade M, Li Y-C, Wahl GM. MDM2, MDMX and p53 in oncogenesis and cancer therapy.  
562 *Nat Rev Cancer* 2013;13(2):83–96; doi: 10.1038/nrc3430.

- 563 14. Kruse J-P, Gu W. Modes of P53 Regulation. *Cell*. 2009.
- 564 15. Olivier M, Hollstein M, Hainaut P. TP53 Mutations in Human Cancers: Origins,  
565 Consequences, and Clinical Use. *Csh Perspect Biol* 2010;2(1):a001008; doi:  
566 10.1101/cshperspect.a001008.
- 567 16. Bolouri H, Farrar JE, Triche T, et al. The molecular landscape of pediatric acute myeloid  
568 leukemia reveals recurrent structural alterations and age-specific mutational interactions. *Nat*  
569 *Med* 2018;24(1):103–112; doi: 10.1038/nm.4439.
- 570 17. Quintás-Cardama A, Hu C, Qutub A, et al. p53 pathway dysfunction is highly prevalent in  
571 acute myeloid leukemia independent of TP53 mutational status. *Leukemia* 2017;31(6):1296–  
572 1305; doi: 10.1038/leu.2016.350.
- 573 18. Hof J, Krentz S, Schewick C van, et al. Mutations and Deletions of the TP53 Gene Predict  
574 Nonresponse to Treatment and Poor Outcome in First Relapse of Childhood Acute  
575 Lymphoblastic Leukemia. *J Clin Oncol* 2011;29(23):3185–3193; doi:  
576 10.1200/jco.2011.34.8144.
- 577 19. Wada M, Bartram CR, Nakamura H, et al. Analysis of p53 mutations in a large series of  
578 lymphoid hematologic malignancies of childhood. *Blood* 1993;82(10):3163–9.
- 579 20. Carvajal LA, Neriah DB, Senecal A, et al. Dual Inhibition of MDMX and MDM2 as a  
580 Therapeutic Strategy in Leukemia. *Science Translational Medicine*. 2018.
- 581 21. Han X, Medeiros LJ, Zhang YH, et al. High Expression of Human Homologue of Murine  
582 Double Minute 4 and the Short Splicing Variant, HDM4-S, in Bone Marrow in Patients With  
583 Acute Myeloid Leukemia or Myelodysplastic Syndrome. *Clin Lymphoma Myeloma*  
584 *Leukemia* 2016;16:S30–S38; doi: 10.1016/j.clml.2016.03.012.
- 585 22. Bueso-Ramos C, Yang Y, deLeon E, et al. The human MDM-2 oncogene is overexpressed  
586 in leukemias. *Blood* 1993;82(9):2617–2623; doi: 10.1182/blood.v82.9.2617.2617.
- 587 23. Gustafsson B, Stål O, Gustafsson B. Overexpression of MDM2 in Acute Childhood  
588 Lymphoblastic Leukemia. *Pediatr Hemat Oncol* 1998;15(6):519–526; doi:  
589 10.3109/08880019809018313.
- 590 24. Han X, Garcia-Manero G, McDonnell TJ, et al. HDM4 (HDMX) is widely expressed in  
591 adult pre-B acute lymphoblastic leukemia and is a potential therapeutic target. *Modern Pathol*  
592 2007;20(1):54–62; doi: 10.1038/modpathol.3800727.
- 593 25. Kaindl U, Morak M, Portsmouth C, et al. Blocking ETV6/RUNX1-induced MDM2  
594 overexpression by Nutlin-3 reactivates p53 signaling in childhood leukemia. *Leukemia*  
595 2014;28(3):600–608; doi: 10.1038/leu.2013.345.
- 596 26. Zhou M, Gu L, Abshire T, et al. Incidence and prognostic significance of MDM2  
597 oncoprotein overexpression in relapsed childhood acute lymphoblastic leukemia. *Leukemia*  
598 2000;14(1):61–67; doi: 10.1038/sj.leu.2401619.



- 599 27. Zhou M, Yeager AM, Smith SD, et al. Overexpression of the MDM2 gene by childhood  
600 acute lymphoblastic leukemia cells expressing the wild-type p53 gene. *Blood*  
601 1995;85(6):1608–14.
- 602 28. Wade M, Wang YV, Wahl GM. The P53 Orchestra: Mdm2 and Mdmx Set the Tone.  
603 *Trends in Cell Biology*. 2010.
- 604 29. Stommel JM, Kimmelman AC, Ying H, et al. Coactivation of Receptor Tyrosine Kinases  
605 Affects the Response of Tumor Cells to Targeted Therapies. *Science* 2007;318(5848):287–  
606 290; doi: 10.1126/science.1142946.
- 607 30. Fielder W, Graeven U, Ergün S, et al. Expression of FLT4 and its ligand VEGF-C in acute  
608 myeloid leukemia. *Leukemia* 1997;11(8):1234–1237; doi: 10.1038/sj.leu.2400722.
- 609 31. Kivivuori S, Siitonen S, Porkka K, et al. Expression of vascular endothelial growth factor  
610 receptor 3 and Tie1 tyrosine kinase receptor on acute leukemia cells. *Pediatr Blood Cancer*  
611 2007;48(4):387–392; doi: 10.1002/pbc.20857.
- 612 32. Nowicki M, Ostalska-Nowicka D, Kaczmarek E, et al. Vascular endothelial growth factor  
613 C—a potent risk factor in childhood acute lymphoblastic leukaemia: an immunocytochemical  
614 approach. *Histopathology* 2006;49(2):170–177; doi: 10.1111/j.1365-2559.2006.02465.x.
- 615 33. Jonge HJM de, Weidenaar AC, Elst A ter, et al. Endogenous Vascular Endothelial Growth  
616 Factor-C Expression Is Associated with Decreased Drug Responsiveness in Childhood Acute  
617 Myeloid Leukemia. *Clin Cancer Res* 2008;14(3):924–930; doi: 10.1158/1078-0432.ccr-07-  
618 1821.
- 619 34. Jonge HJM de, Valk PJM, Veeger NJGM, et al. High VEGFC expression is associated  
620 with unique gene expression profiles and predicts adverse prognosis in pediatric and adult  
621 acute myeloid leukemia. *Blood* 2010;116(10):1747–1754; doi: 10.1182/blood-2010-03-  
622 270991.
- 623 35. Dias S, Choy M, Alitalo K, et al. Vascular endothelial growth factor (VEGF)–C signaling  
624 through FLT-4 (VEGFR-3) mediates leukemic cell proliferation, survival, and resistance to  
625 chemotherapy. *Blood* 2002;99(6):2179–2184; doi: 10.1182/blood.v99.6.2179.
- 626 36. Polo A de, Luo Z, Gerarduzzi C, et al. AXL receptor signalling suppresses p53 in  
627 melanoma through stabilization of the MDMX–MDM2 complex. *J Mol Cell Biol*  
628 2017;9(2):154–165; doi: 10.1093/jmcb/mjw045.
- 629 37. Calabrese V, Mallette FA, Deschênes-Simard X, et al. SOCS1 Links Cytokine Signaling  
630 to p53 and Senescence. *Mol Cell* 2009;36(5):754–767; doi: 10.1016/j.molcel.2009.09.044.
- 631 38. Tang Z, Li C, Kang B, et al. GEPIA: a web server for cancer and normal gene expression  
632 profiling and interactive analyses. *Nucleic Acids Res* 2017;45(Web Server issue):W98–  
633 W102; doi: 10.1093/nar/gkx247.
- 634 39. Chandrashekar DS, Karthikeyan SK, Korla PK, et al. UALCAN: An update to the  
635 integrated cancer data analysis platform. *Neoplasia* 2022;25:18–27; doi:  
636 10.1016/j.neo.2022.01.001.

- 637 40. Chapuy B, Stewart C, Dunford AJ, et al. Molecular subtypes of diffuse large B cell  
638 lymphoma are associated with distinct pathogenic mechanisms and outcomes. *Nat Med*  
639 2018;24(5):679–690; doi: 10.1038/s41591-018-0016-8.
- 640 41. Lohr JG, Stojanov P, Lawrence MS, et al. Discovery and prioritization of somatic  
641 mutations in diffuse large B-cell lymphoma (DLBCL) by whole-exome sequencing. *Proc*  
642 *National Acad Sci* 2012;109(10):3879–3884; doi: 10.1073/pnas.1121343109.
- 643 42. Morin RD, Mungall K, Pleasance E, et al. Mutational and structural analysis of diffuse  
644 large B-cell lymphoma using whole-genome sequencing. *Blood* 2013;122(7):1256–1265; doi:  
645 10.1182/blood-2013-02-483727.
- 646 43. Hoadley KA, Yau C, Hinoue T, et al. Cell-of-Origin Patterns Dominate the Molecular  
647 Classification of 10,000 Tumors from 33 Types of Cancer. *Cell* 2018;173(2):291-304.e6; doi:  
648 10.1016/j.cell.2018.03.022.
- 649 44. Reddy A, Zhang J, Davis NS, et al. Genetic and Functional Drivers of Diffuse Large  
650 B Cell Lymphoma. *Cell* 2017;171(2):481-494.e15; doi: 10.1016/j.cell.2017.09.027.
- 651 45. Zhang J, McCastlain K, Yoshihara H, et al. Deregulation of DUX4 and ERG in acute  
652 lymphoblastic leukemia. *Nat Genet* 2016;48(12):1481–1489; doi: 10.1038/ng.3691.
- 653 46. Andersson AK, Ma J, Wang J, et al. The landscape of somatic mutations in infant MLL-  
654 rearranged acute lymphoblastic leukemias. *Nat Genet* 2015;47(4):330–337; doi:  
655 10.1038/ng.3230.
- 656 47. Alexander TB, Gu Z, Iacobucci I, et al. The genetic basis and cell of origin of mixed  
657 phenotype acute leukaemia. *Nature* 2018;562(7727):373–379; doi: 10.1038/s41586-018-  
658 0436-0.
- 659 48. Villiard É, Brinkmann H, Moiseeva O, et al. Urodele p53 tolerates amino acid changes  
660 found in p53 variants linked to human cancer. *Bmc Evol Biol* 2007;7(1):180–180; doi:  
661 10.1186/1471-2148-7-180.
- 662 49. Foo RS-Y, Chan LKW, Kitsis RN, et al. Ubiquitination and Degradation of the Anti-  
663 apoptotic Protein ARC by MDM2\*. *J Biol Chem* 2007;282(8):5529–5535; doi:  
664 10.1074/jbc.m609046200.
- 665 50. Shadfan M, Lopez-Pajares V, Yuan Z-M. MDM2 and MDMX: Alone and together in  
666 regulation of p53. *Transl Cancer Res* 2012;1(2):88–89.
- 667 51. Gerarduzzi C, Polo A de, Liu X-S, et al. Human epidermal growth factor receptor 4  
668 (Her4) Suppresses p53 Protein via Targeting the MDMX-MDM2 Protein Complex  
669 IMPLICATION OF A NOVEL MDMX SER-314 PHOSPHOSITE\*. *J Biol Chem*  
670 2016;291(50):25937–25949; doi: 10.1074/jbc.m116.752303.
- 671 52. Xu AM, Huang PH. Receptor Tyrosine Kinase Coactivation Networks in Cancer. *Cancer*  
672 *Res* 2010;70(10):3857–3860; doi: 10.1158/0008-5472.can-10-0163.

673 53. Reyes J, Chen J-Y, Stewart-Ornstein J, et al. Fluctuations in p53 Signaling Allow Escape  
674 from Cell-Cycle Arrest. *Mol Cell* 2018;71(4):581-591.e5; doi: 10.1016/j.molcel.2018.06.031.

675 54. Otto T, Sicinski P. Cell cycle proteins as promising targets in cancer therapy. *Nat Rev*  
676 *Cancer* 2017;17(2):93–115; doi: 10.1038/nrc.2016.138.

677

678

679

680

681 **FIGURE LEGENDS**

682 **Figure 1: FLT4 and its ligand VEGF-C are upregulated in patients and are associated**  
683 **with cancer progression. A)** FLT4 and VEGF-C mRNA expression in healthy and Diffuse  
684 Large B-cell Lymphoma (DLBC) patients. The data were generated using Gene Expression  
685 Profiling Interactive Analysis (GEPIA). DLBC (n=47), Healthy (n=337), \*p<0.01 (Log<sub>2</sub>FC  
686 0.6). **B)** FLT4 expression in DLBC patients at individual cancer stages. The data were generated  
687 using the ULCAN-TCGA database. Stage 1 (n=8), stage 2 (n=17), stage 3 (n=4), Stage 4  
688 (n=12). \*p<0.05 vs. stage 1.

689

690 **Figure 2: FLT4 overexpression negatively regulates p53 expression and subsequently**  
691 **downregulates its target genes. A)** The frequency of p53 mutation in Diffuse Large B Cell  
692 lymphoma (DLBC) patients (*DFCI, Nat Med, 2018*), (*Broad, PNAS, 2012*), (*BCGSC, Blood,*  
693 *2013*), (*TCGA, PanCancer Atlas*), (*Duke, Cell, 2017*), ALL patients (*St Jude, Nat Genet, 2016*),  
694 (*St Jude, Nat Genet, 2015*), and pediatric ALL patients (TARGET, 2018) – across public  
695 datasets in <https://www.cbioportal.org/>. **B)** U2OS cells were transfected with an empty or FLT4  
696 expression plasmid along with a pg13 luciferase reporter vector or a luciferase reporter for p21  
697 or MDM2 to determine p53 target genes activity. **C)** U2OS cells were transfected with different  
698 combinations of FLT4, MDM2 and MDMX plasmids along with pg13 luciferase reporter vector  
699 to determine endogenous p53 under genotoxic conditions (5'FU = 375 μM). **D)** HEK293T cells  
700 were transfected with various amounts of FLT4 expression plasmids for 24h. The cell lysates  
701 were blotted for the indicated antibodies. **E)** HEK293T cells were transfected with a  
702 combination of FLT4, MDMX and MDM2 expression plasmids for 24h. The cell lysates were  
703 blotted for the indicated antibodies. **F)** U2OS cells were transfected with a combination of  
704 FLT4, MDMX or MDM2 expression plasmids for 24h. The cell lysates were blotted for the

705 indicated antibodies. **G)** U2OS cells were transfected with a combination of FLT4, MDMX,  
706 wild type MDM2 or mutant MDM2 C464A expression plasmids for 24h. The cell lysates were  
707 blotted for the indicated antibodies. \* $p < 0.05$ , \*\*\*\* $p < 0.0001$ .

708

709 **Figure 3: FLT4 overexpression increases the stability of MDM2/MDMX complex and**  
710 **relocalizes it in the cytoplasm.** U2OS cells were transfected with a combination of FLT4,  
711 MDMX and MDM2 expression plasmids and immunostained for MDMX (Green) and MDM2  
712 (Red), while the nuclei were stained with DAPI. Scale bar: 20  $\mu\text{m}$ .

713

714 **Figure 4: FLT4 activation leads to MDMX S314 phosphorylation through the activation**  
715 **CDK4/6 pathway. A)** HEK293T cells were transfected with a combination of MDMX, Myc-  
716 MDM2 with or without FLT4 and harvested 24h later for immunoprecipitation (IP) with Myc  
717 antibody-conjugated beads. Whole Cell Extract (WCE) and Myc IP samples were subjected to  
718 Western Blot analysis with the indicated antibodies. **B)** HEK293T cells were transfected with  
719 various combinations of wild type MDMX, mutant MDMX S314A, MDM2 and FLT4  
720 plasmids. After 24h of transfection, cells were harvested, and subjected to Western Blot analysis  
721 using the indicated antibodies. LE, low exposure. HE, high exposure. **C)** HEK293T cells were  
722 transfected with either wild type MDMX or mutant MDMX S314A in combination with Myc-  
723 MDM2 and FLT4 plasmids. After 24h of transfection, cell lysates were harvested for IP with  
724 Myc-antibody-conjugated beads. WCE and Myc IP samples were subjected to Western Blot  
725 analysis with the indicated antibodies. **D)** HEK293T cells were transfected with a combination  
726 of MDM2, MDMX and FLT4 plasmids for 24h, then treated with various concentrations of  
727 Palbociclib for 24h. Cells were harvested and analyzed by Western Blot using the indicated  
728 antibodies.

729

730 **Figure 5: FLT4 stimulation with VEGF-C requires CDK4/6 to stabilize the**  
731 **MDM2/MDMX complex and p53 decrease in leukemic cells.** A) FLT4 expression in  
732 leukemic cell lines. Published RNA sequencing data of various *in vitro* ALL models were  
733 analyzed for FLT4 expression. The abundance in 'Transcript Per Million' (TPM) was reported  
734 as the sum of the TPM values of all its protein-coding transcripts. The threshold level to detect  
735 the presence of a transcript for a particular gene was set to  $\geq 1$  TPM. B) REH cells were treated  
736 with the FLT4 ligand, VEGF-C (100 ng/mL), for 2h or 3h and then harvested for Western Blot  
737 analysis using the indicated antibodies. C) REH cells were pre-treated with the FLT4 inhibitor,  
738 MAZ51 (5  $\mu$ M), for 30 min, then treated with 100 ng/ml of VEGF-C for 25 or 30 min. Cell  
739 lysates were collected for Western Blot analysis using the indicated antibodies. D) REH cells  
740 were transduced with FLT4 (vFLT4) or empty vector, then harvested and subjected to Western  
741 Blot with the indicated antibodies. E) REH transduced cells were pre-treated for 24h with the  
742 CDK4/6 inhibitor, Palbociclib (2.5  $\mu$ M), then harvested for Western Blotted using the indicated  
743 antibodies.

744

745 **Figure 6: FLT4 overexpression decreases p53 and promotes cell survival and resistance**  
746 **to chemotherapy.** A) REH cells transduced with FLT4 (vFLT4) or empty vector were seeded  
747 in a 6-well plate with a complete medium and counted every day for five consecutive days. B)  
748 REH transduced cells were plated in 1.2% methyl-cellulose. After two weeks of culture,  
749 colonies consisting of at least 50 cells were counted using an inverted microscope. C) REH  
750 transduced cells were treated with Doxorubicin (50 nM, 5h), then harvested and subjected to  
751 Western Blotting for the indicated antibodies. D, E) REH transduced cells were treated with 50  
752 nM (D) or various amounts (E) of Doxorubicin for 48h. Cells were stained with Annexin V and

753 DAPI , and apoptosis was measured by flow cytometry. **F)** REH transduced cells were treated  
754 with Etoposide (0.25  $\mu$ M, 3h), then harvested and subjected to Western Blotting for the  
755 indicated antibodies. **G, H)** REH transduced cells were treated with 0.25  $\mu$ M (G) or various  
756 amounts (H) of Etoposide for 24h. Cells were stained with Annexin V and DAPI, and apoptosis  
757 was measured by flow cytometry. \* $p < 0.05$ , \*\* $p < 0.01$ .

758

759 **Figure 7: Inhibition of CDK4/6 prevents FLT4- induction of proliferation and -resistance**  
760 **to DNA damaging apoptosis.** **A)** REH cells transduced with FLT4 (vFLT4) or empty vector  
761 were seeded in a 6-well plate in complete medium, then treated with the CDK4/6 inhibitor,  
762 Palbociclib (1  $\mu$ M), at day 0 and counted every day for five consecutive days. **B)** REH  
763 transduced cells (vFLT4) were pre-treated with Palbociclib (1  $\mu$ M) for 24h and then treated  
764 with 50 nM of Doxorubicin for 48h. Cells were stained with Annexin V and DAPI, and  
765 apoptosis was measured by flow cytometry. \*\* $p < 0.01$ , \*\*\* $p < 0.001$ , \*\*\*\* $p < 0.0001$ .

766

767 **Figure 8: Schematic representation of FLT4-mediated MDM2/MDMX complex**  
768 **stabilization and suppression of p53 activity.** VEGF-C triggers FLT4 activation, leading to  
769 CDK4/6 activation, which phosphorylates MDMX on Ser-314. As a result, MDMX levels  
770 increase and bind to MDM2, stabilizing the MDM2/MDMX complex. This complex binds to  
771 p53, facilitating its suppression via reduced transcriptional activity or enhanced export to the  
772 cytoplasm for proteasome degradation. Consequently, p53 inactivation promotes their survival,  
773 proliferation, and resistance to chemotherapy-induced apoptosis. *The figure was created in*  
774 *BioRender.com*

775

776 **Supplementary Figure 1** : U2OS cells were transfected with various amounts of FLT4  
777 expression plasmids for 24h. The cell lysates were blotted for the indicated antibodies.

778

779 **Supplementary Figure 2**: HEK293FT cells were transfected with MDMX WT or MDMX  
780 S314A expression plasmids for 24h. The cell lysates were blotted for the indicated antibody.

781

782 **Supplementary Figure 3**: **A)** At various time points, REH cells were treated with the FLT4  
783 ligand, VEGF-C (100 ng/mL), then harvested and subjected to Western Blot with the indicated  
784 antibodies. **B)** REH cells were pre-treated for 30 min with the FLT4 inhibitor, MAZ51 (5  $\mu$ M),  
785 then treated with 100 ng/ml of VEGF-C for 2h. The cells were harvested for Western Blot with  
786 the indicated antibodies.

787



# Figures

## Figure 1

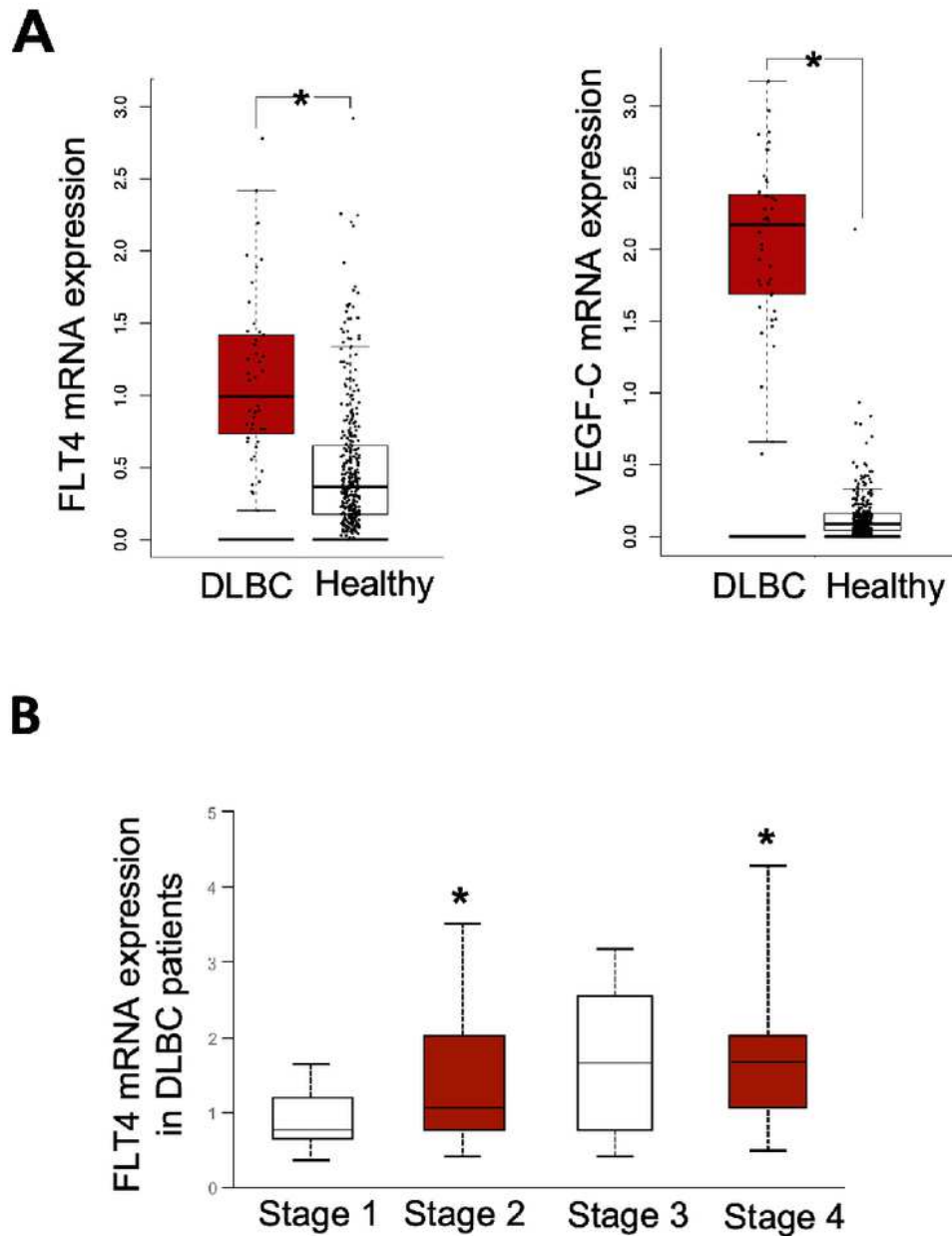
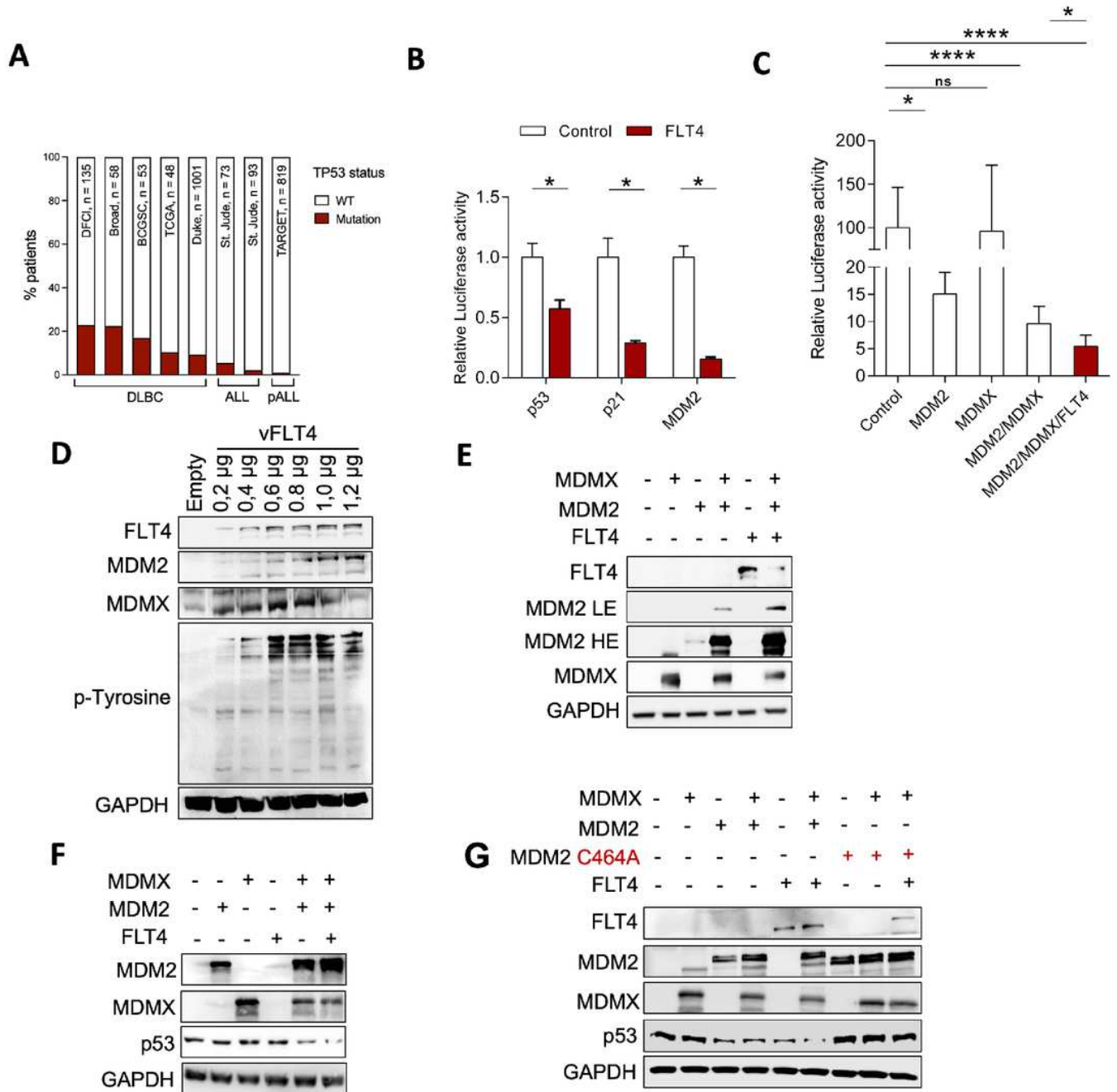


Figure 1

FLT4 and its ligand VEGF-C are upregulated in patients and are associated with cancer progression. A) FLT4 and VEGF-C mRNA expression in healthy and Diffuse

Large B-cell Lymphoma (DLBC) patients. The data were generated using Gene Expression Profiling Interactive Analysis (GEPIA). DLBC (n=47), Healthy (n=337), \*p<0.01 (Log2FC 0.6). B) FLT4 expression in DLBC patients at individual cancer stages. The data were generated using the ULCAN-TCGA database. Stage 1 (n=8), stage 2 (n=17), stage 3 (n=4), Stage 4 (n=12). \*p<0.05 vs. stage 1.

**Figure 2**



**Figure 2**

FLT4 overexpression negatively regulates p53 expression and subsequently downregulates its target genes. A) The frequency of p53 mutation in Diffuse Large B Cell lymphoma (DLBC) patients (DFCI, Nat Med, 2018), (Broad, PNAS, 2012), (BCGSC, Blood, 2013), (TCGA, PanCancer Atlas), (Duke, Cell, 2017), ALL patients (St Jude, Nat Genet, 2016), (St Jude, Nat Genet, 2015), and pediatric ALL patients (TARGET, 2018) – across public datasets in <https://www.cbioportal.org/>. B) U2OS cells were transfected with an empty or FLT4 expression plasmid along with a pg13 luciferase reporter vector or a luciferase reporter for p21 or MDM2 to determine p53 target genes activity. C) U2OS cells were transfected with different combinations of FLT4, MDM2 and MDMX plasmids along with pg13 luciferase reporter vector to determine endogenous p53 under genotoxic conditions (5'FU = 375  $\mu$ M). D) HEK293T cells were transfected with various amounts of FLT4 expression plasmids for 24h. The cell lysates were blotted for the indicated antibodies. E) HEK293T cells were transfected with a combination of FLT4, MDMX and MDM2 expression plasmids for 24h. The cell lysates were blotted for the indicated antibodies. F) U2OS cells were transfected with a combination of FLT4, MDMX or MDM2 expression plasmids for 24h. The cell lysates were blotted for the indicated antibodies. G) U2OS cells were transfected with a combination of FLT4, MDMX, wild type MDM2 or mutant MDM2 C464A expression plasmids for 24h. The cell lysates were blotted for the indicated antibodies. \*p<0.05, \*\*\*\*p<0.0001.

# Figure 3

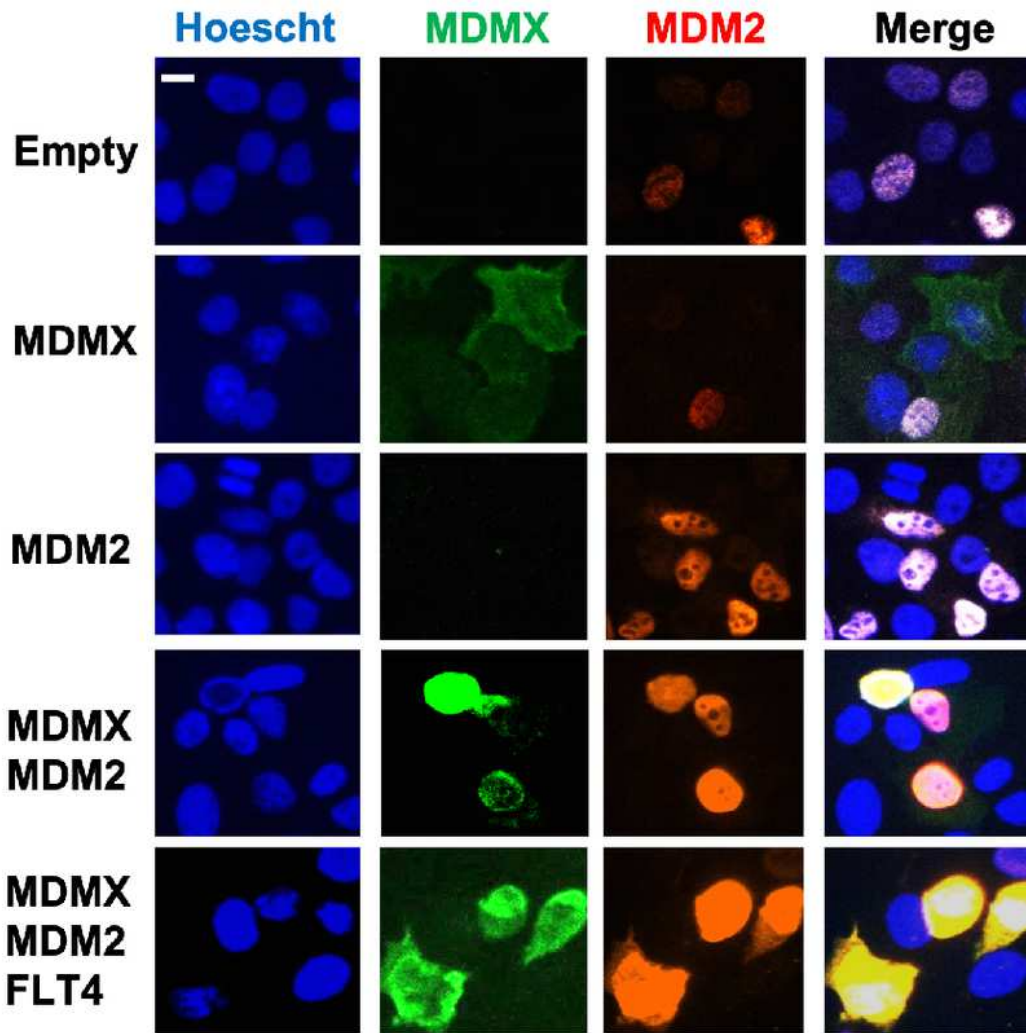
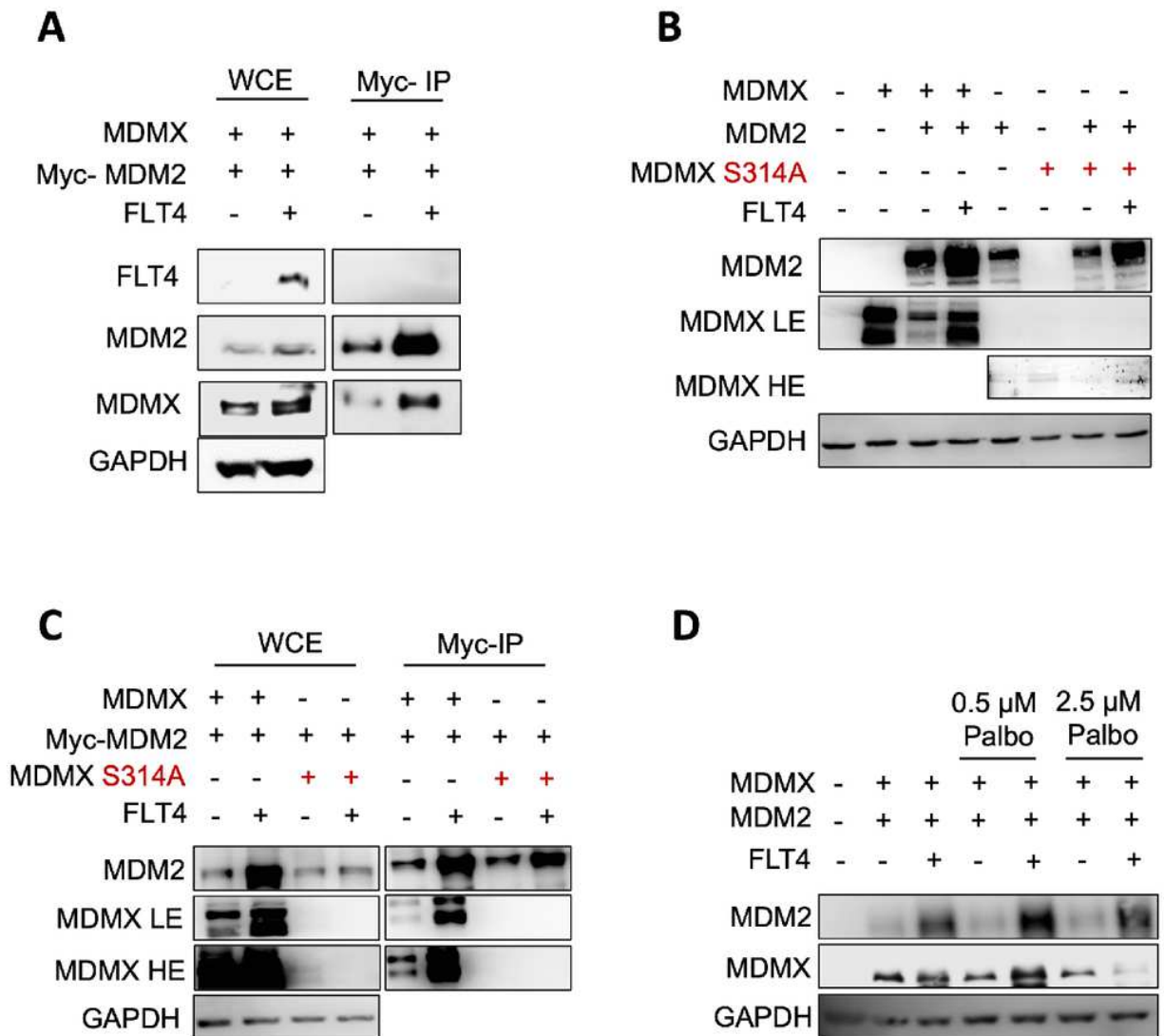


Figure 3

FLT4 overexpression increases the stability of MDM2/MDMX complex and relocalizes it in the cytoplasm. U2OS cells were transfected with a combination of FLT4, MDMX and MDM2 expression plasmids and immunostained for MDMX (Green) and MDM2

(Red), while the nuclei were stained with DAPI. Scale bar: 20  $\mu$ m.

## Figure 4



## Figure 4

FLT4 activation leads to MDMX S314 phosphorylation through the activation

CDK4/6 pathway. A) HEK293T cells were transfected with a combination of MDMX, Myc-MDM2 with or without FLT4 and harvested 24h later for immunoprecipitation (IP) with Myc antibody-conjugated beads. Whole Cell Extract (WCE) and Myc IP samples were subjected to Western Blot analysis with the indicated antibodies. B) HEK293T cells were transfected with various combinations of wild type MDMX, mutant MDMX S314A, MDM2 and FLT4

plasmids. After 24h of transfection, cells were harvested, and subjected to Western Blot analysis using the indicated antibodies. LE, low exposure. HE, high exposure. C) HEK293T cells were transfected with either wild type MDMX or mutant MDMX S314A in combination with Myc-MDM2 and FLT4 plasmids. After 24h of transfection, cell lysates were harvested for IP with Myc-antibody-conjugated beads. WCE and Myc IP samples were subjected to Western Blot analysis with the indicated antibodies. D) HEK293T cells were transfected with a combination of MDM2, MDMX and FLT4 plasmids for 24h, then treated with various concentrations of Palbociclib for 24h. Cells were harvested and analyzed by Western Blot using the indicated antibodies.

# Figure 5

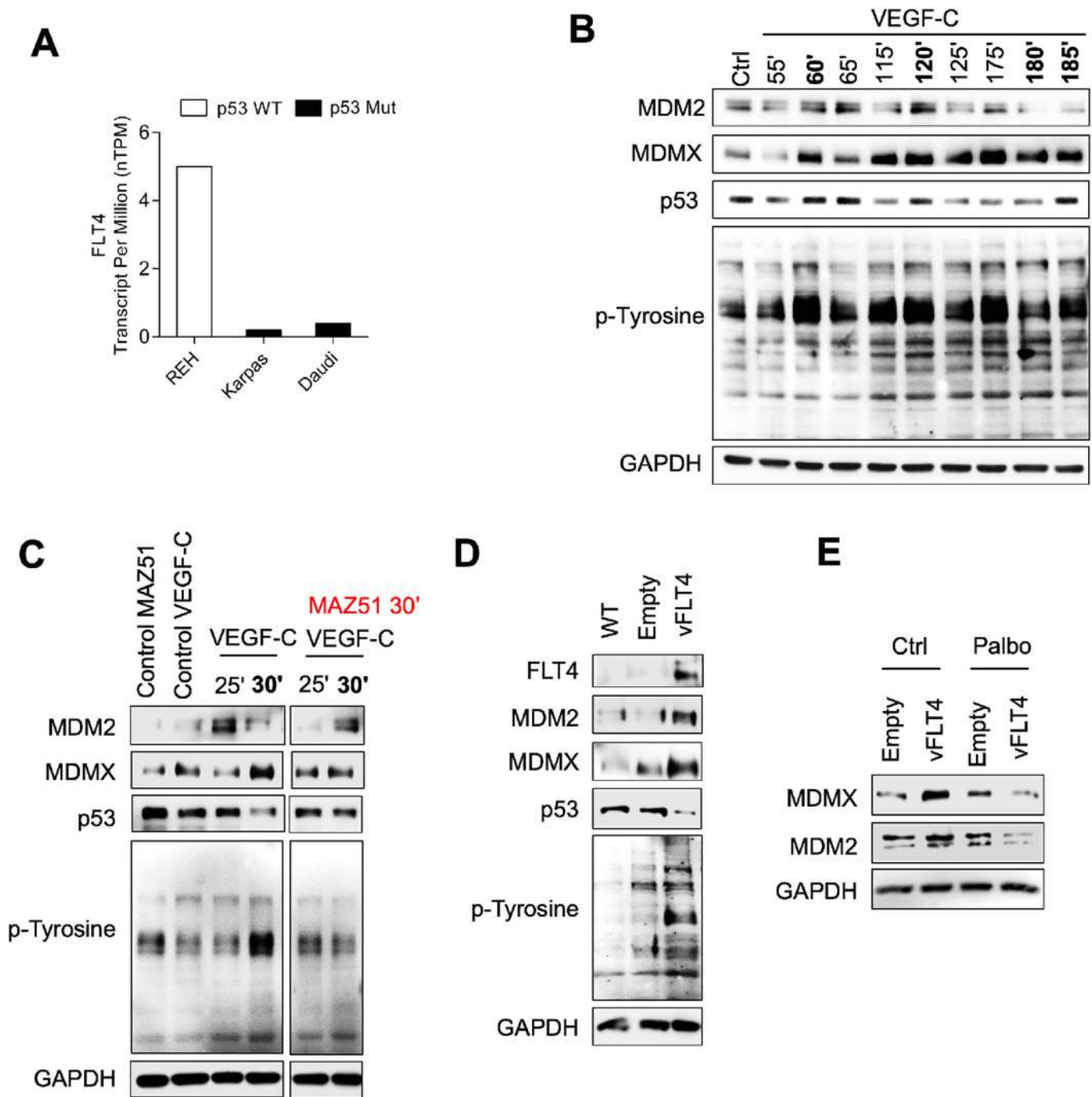


Figure 5

FLT4 stimulation with VEGF-C requires CDK4/6 to stabilize the MDM2/MDMX complex and p53 decrease in leukemic cells. A) FLT4 expression in leukemic cell lines. Published RNA sequencing data of various in vitro ALL models were

analyzed for FLT4 expression. The abundance in 'Transcript Per Million' (TPM) was reported as the sum of the TPM values of all its protein-coding transcripts. The threshold level to detect the presence of a transcript for a particular gene was set to  $\geq 1$  TPM. B) REH cells were treated with the FLT4 ligand, VEGF-C (100 ng/mL), for 2h or 3h and then harvested for Western Blot analysis using the indicated antibodies. C) REH cells were pre-treated with the FLT4 inhibitor, MAZ51 (5  $\mu$ M), for 30 min, then treated with 100 ng/ml of VEGF-C for 25 or 30 min. Cell lysates were collected for Western Blot analysis using the indicated antibodies. D) REH cells were transduced with FLT4 (vFLT4) or empty vector, then harvested and subjected to Western Blot with the indicated antibodies. E) REH transduced cells were pre-treated for 24h with the CDK4/6 inhibitor, Palbociclib (2.5  $\mu$ M), then harvested for Western Blotted using the indicated antibodies.



**Figure 6**

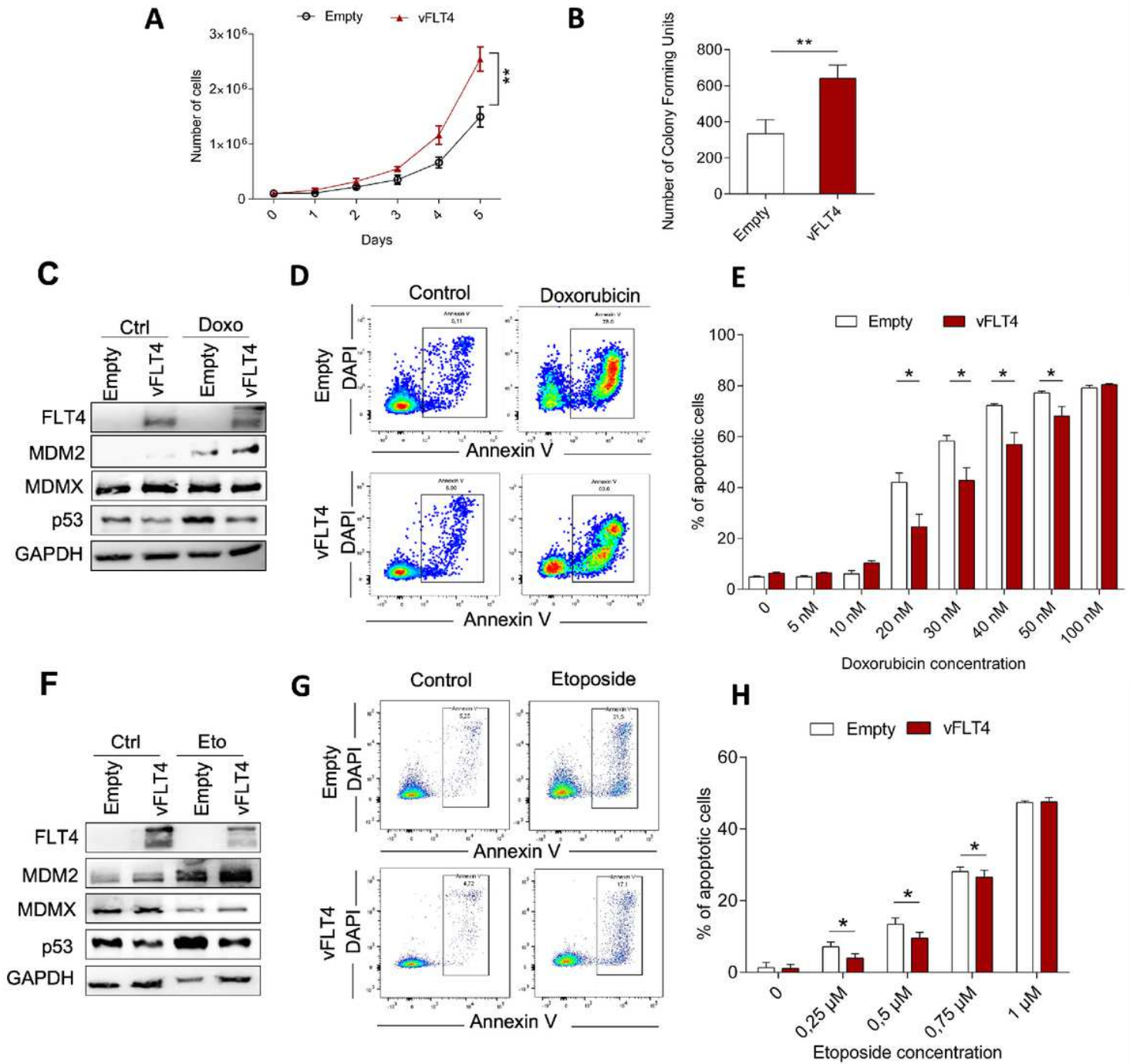


**Figure 6**

FLT4 overexpression decreases p53 and promotes cell survival and resistance

to chemotherapy. A) REH cells transduced with FLT4 (vFLT4) or empty vector were seeded

in a 6-well plate with a complete medium and counted every day for five consecutive days. B)

REH transduced cells were plated in 1.2% methyl-cellulose. After two weeks of culture,

colonies consisting of at least 50 cells were counted using an inverted microscope. C) REH transduced cells were treated with Doxorubicin (50 nM, 5h), then harvested and subjected to Western Blotting for the indicated antibodies. D, E) REH transduced cells were treated with 50 nM (D) or various amounts (E) of Doxorubicin for 48h. Cells were stained with Annexin V and DAPI, and apoptosis was measured by flow cytometry. F) REH transduced cells were treated with Etoposide (0.25  $\mu$ M, 3h), then harvested and subjected to Western Blotting for the indicated antibodies. G, H) REH transduced cells were treated with 0.25  $\mu$ M (G) or various amounts (H) of Etoposide for 24h. Cells were stained with Annexin V and DAPI, and apoptosis was measured by flow cytometry. \* $p < 0.05$ , \*\* $p < 0.01$ .

**Figure 7**

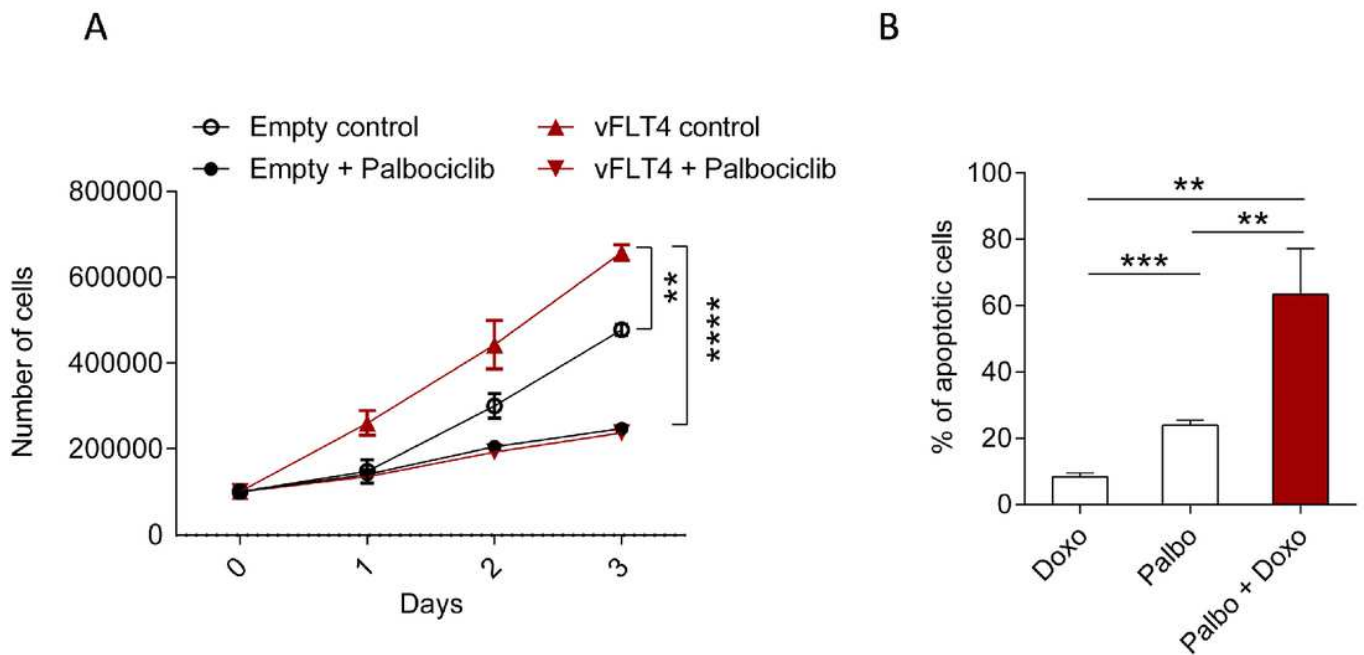


**Figure 7**

Inhibition of CDK4/6 prevents FLT4- induction of proliferation and -resistance to DNA damaging apoptosis. A) REH cells transduced with FLT4 (vFLT4) or empty vector were seeded in a 6-well plate in complete medium, then treated with the CDK4/6 inhibitor, Palbociclib (1  $\mu$ M), at day 0 and counted every day for five consecutive days. B) REH

transduced cells (vFLT4) were pre-treated with Palbociclib (1  $\mu$ M) for 24h and then treated with 50 nM of Doxorubicin for 48h. Cells were stained with Annexin V and DAPI, and apoptosis was measured by flow cytometry. \*\* $p < 0.01$ , \*\*\* $p < 0.001$ , \*\*\*\* $p < 0.0001$ .

## Figure 8

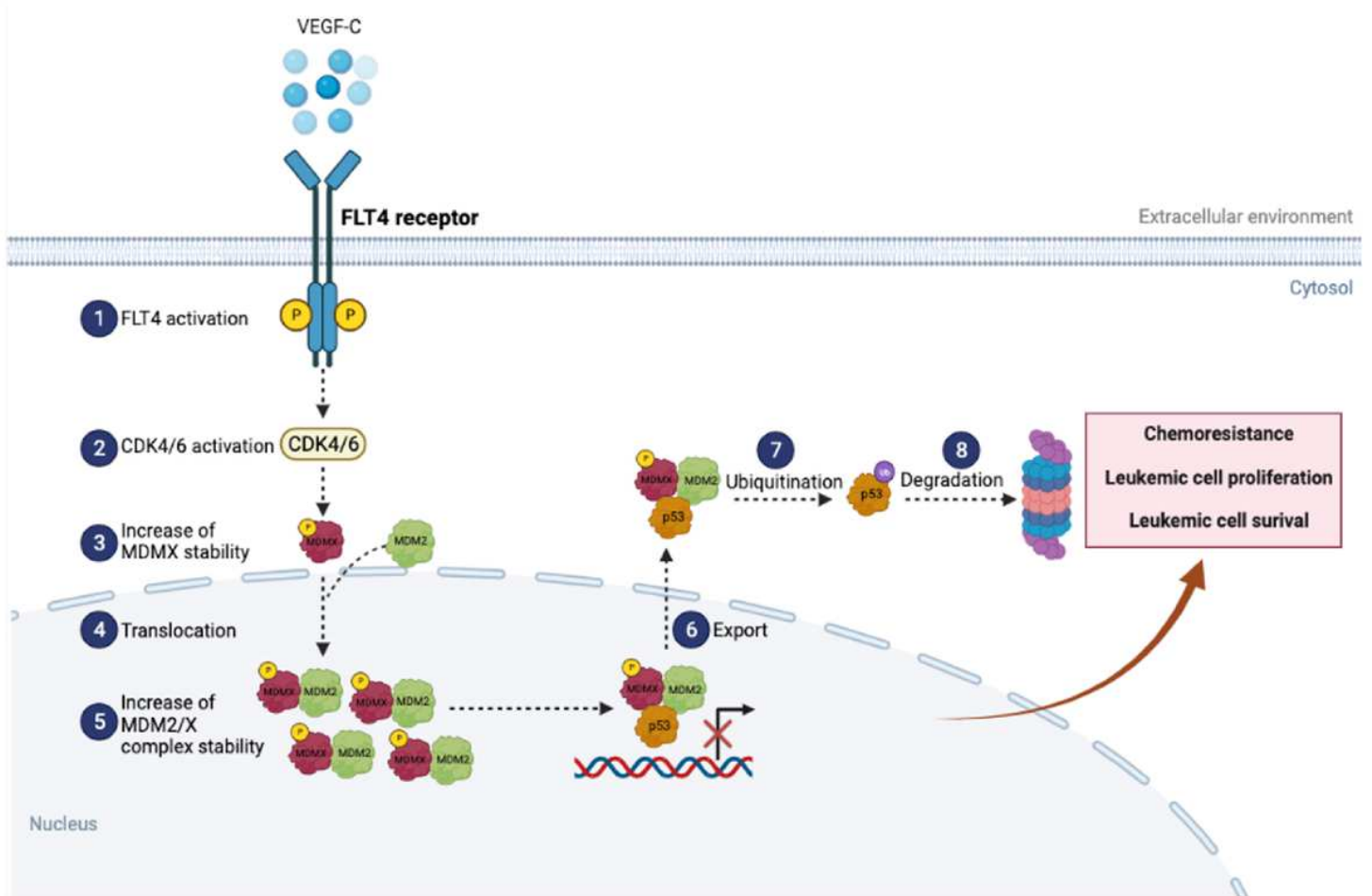


## Figure 8

Schematic representation of FLT4-mediated MDM2/MDMX complex

stabilization and suppression of p53 activity. VEGF-C triggers FLT4 activation, leading to CDK4/6 activation, which phosphorylates MDMX on Ser-314. As a result, MDMX levels increase and bind to MDM2, stabilizing the MDM2/MDMX complex. This complex binds to p53, facilitating its suppression via reduced transcriptional activity or enhanced export to the cytoplasm for proteasome degradation. Consequently, p53 inactivation promotes their survival,

proliferation, and resistance to chemotherapy-induced apoptosis. The figure was created in

BioRender.com

## Supplementary Files

This is a list of supplementary files associated with this preprint. Click to download.

- [SupplementaryFigure1.pdf](#)
- [SupplementaryFigure2.pdf](#)
- [SupplementaryFigure3.pdf](#)